NJC

Accepted Manuscript

Volume 40 | Number 1 | January 2016 | Pages 1–846

NJC

New Journal of Chemistry
www.rsc.org/njc

A journal for new directions in chemistry

ISSN 1144-0546

ROYAL SOCIETY OF CHEMISTRY

PAPER
Jason B. Benedict et al
The role of atropisomers on the photo-reactivity and fatigue of diarylethene-based metal–organic frameworks

cnrs

This is an Accepted Manuscript, which has been through the Royal Society of Chemistry peer review process and has been accepted for publication.

Accepted Manuscripts are published online shortly after acceptance, before technical editing, formatting and proof reading. Using this free service, authors can make their results available to the community, in citable form, before we publish the edited article. We will replace this Accepted Manuscript with the edited and formatted Advance Article as soon as it is available.

You can find more information about Accepted Manuscripts in the author guidelines.

Please note that technical editing may introduce minor changes to the text and/or graphics, which may alter content. The journal's standard Terms & Conditions and the ethical guidelines, outlined in our author and reviewer resource centre, still apply. In no event shall the Royal Society of Chemistry be held responsible for any errors or omissions in this Accepted Manuscript or any consequences arising from the use of any information it contains.

rsc.li/njc

New thiosemicarbazide and dithiocarbazate based oxidovanadium(IV) and dioxidovanadium(V) complexes. Reactivity and catalytic potential

Mannar R. Maurya*[,a], Bithika Sarkar[a], Amit Kumar[b,c], Nádia Ribeiro [b], Aistè Miliute [b] and J. C. Pessoa*[,b]

[a]*Department of Chemistry, Indian Institute of Technology Roorkee, Roorkee 247 667, India,*
Email: rkmanfcy@iitr.ernet.in

[b]*Centro de Química Estrutural, Departamento de Engenharia Química, Instituto Superior Técnico, Universidade Técnica de Lisboa, Av Rovisco Pais, 1049-001 Lisboa, Portugal. Email: joao.pessoa@ist.utl.pt*

[c]*Center for Nano & Material Science, Jain (Deemed-to-be-University), Jakkasandra Post, Bangalore 562112, Karnataka, India.*

Abstract

The Schiff bases {H_3dfmp-(smdt)$_2$} (**I**), {H_3dfmp-(sbdt)$_2$} (**II**) and {H_3dfmp-(tsc)$_2$}(**III**) are synthesized by reaction of 2,6-diformyl-4-methylphenol (H_3dfmp) and S-methyldithiocarbazate (smdt), S-benzyldithiocarbazate (sbdt) and thiosemicarbazide (tsc), respectively. Addition of [$V^{IV}O$(acac)$_2$] to solutions of these compounds in methanol leads to the formation of the oxidovanadium(IV) complexes [$V^{IV}O${Hdfmp-(smdt)$_2$(CH$_3$OH)}] (**1**), [$V^{IV}O${Hdfmp-(sbdt)$_2$(CH$_3$OH)}] (**2**) and [$V^{IV}O${Hdfmp-(tsc)$_2$(CH$_3$OH)}] (**3**). All these $V^{IV}O$-compounds can be oxidized to the corresponding dioxidovanadium(V) (V^VO_2) complexes in methanolic solution upon aerial oxidation in the presence of KOH. The isolated compounds are K[V^VO_2{Hdfmp-(smdt)$_2$}] (**4**), K[V^VO_2{Hdfmp-(sbdt)$_2$}] (**5**) and K[V^VO_2{Hdfmp-(tsc)$_2$}] (**6**). The Cs$^+$ salt of these complexes i.e. Cs[V^VO_2{Hdfmp-(smdt)$_2$}] (**7**), Cs[V^VO_2{Hdfmp-(sbdt)$_2$}] (**8**) and Cs[V^VO_2{Hdfmp-(tsc)$_2$}] (**9**) are prepared similarly in the presence of CsOH. All these compounds are characterized by various spectroscopic techniques like FT-IR, UV-Visible, ^{1}H and ^{51}V NMR and thermal studies. IR spectral data confirm the coordination of ligands through the azomethine nitrogen, sulphur and the phenolic oxygen atoms to the metal. These complexes show excellent catalytic activity and selectivity for the oxidation of benzyl alcohol and ethylbenzene in the presence of H_2O_2 as an oxidant. Various parameters such as amount of catalyst and oxidant, reaction time, reaction temperature and solvent were taken into

1

consideration to optimize these catalytic oxidations. Compound **7** was also remarkably efficient and selective in the catalytic oxidation of primary and secondary alcohols to the corresponding aldehyde/ketone, as well as of several aromatic compounds such as toluene, benzene, cumene and tetralin.

Keywords: Oxidovanadium(IV) complexes; dioxidovanadium(V) complexes; polydentate ligands; spectroscopic studies; catalytic oxidations.

Introduction

Within the areas of vanadium chemistry and biological chemistry, in addition to therapeutic applications,[1-12] one of the most active areas of research has been the study of the catalytic potential of vanadium complexes,[13-17] namely catalytic oxidations.[18-28] Polynuclear metal complexes with phenol-based polynucleating ligands have been reviewed by Ambrosi et al.[29] Such a class of ligands has attracted attention of researchers because they are able to simultaneously bind two or more metal ions. Transition metal ions such as Mn(III, IV), Ni(II), Co(II), Cu(II) Zn(II) etc. generally form phenoxido bridged binuclear complexes with ligands derived from 2,6-diformyl-4-methylphenol. Such oxidophenoxidovanadium(IV/V) complexes of general formula $[V_2O_3L]$ have only been isolated with the tribasic symmetrical ONN(O)NNO-coordinating heptadentate ligand 2,6-bis[{{(2-hydroxybenzyl)(N′,N′-(dimethylamino)ethyl)}amino}methyl]-4-methylphenol and its derivatives.[30] Reducing the functionalities to dibasic symmetrical ON(O)NO pentadentate resulted in the formation of mainly monodentate vanadium complexes leaving two coordination sites free from coordination.[31] However, the additional suitable coordination site present on each pendent arm led to the formation of polynuclear complex.[24,31] Some of us also reported the characterization of vanadium complexes of 2,6-diformyl-4-methylphenol derived polydentate ligands mainly in solution[31] as well as $V^{IV}O$-mononuclear complexes.[24]

Continuing our efforts in this field, we have now designed dibasic symmetrical SN(O)NS pentadentate ligands i.e. thiohydrazones of 2,6-diformyl-4-methylphenol (Scheme 1) and prepared a series of monodentate oxidovanadium(IV)- ($V^{IV}O$-), oxidovanadium(V)- (V^VO-) and dioxidovanadium(V)- (V^VO_2-) complexes. Their characterization, reactivity and catalytic performance are reported.

Direct oxidation of the abundant and cheap hydrocarbons and alcohols to the corresponding aldehydes and ketones are processes of major important transformations in organic synthesis, since these oxidation products are very important intermediates for the generation of the useful primary or special chemicals, as well as highly valued fine chemicals, agrochemicals, pharmaceutical and compounds for perfumes industry.

Acetophenone is an important intermediate which is extensively used for the synthesis of some perfumes, pharmaceuticals, resins, alcohols, esters, aldehydes and tear gas, and as a solvent for cellulose ethers. Therefore, there has been significant interest in the development of sustainable and efficient processes for the production of acetophenone from ethylbenzene. The oxidation process of ethylbenzene to acetophenone with H_2O_2 as the oxidant has been reported extensively.[16,21] In addition to dioxygen, aqueous hydrogen peroxide (H_2O_2) is the ultimate green oxidant since it produces water as the sole by-product, and it is easy to be dealt with after reactions. The latest studies have therefore been paying attention on the catalytic oxidation of ethylbenzene with H_2O_2 as the terminal oxidant.[16]

In this work we explore the performance of a set of $V^{IV}O$- and $V^{V}O_2$-complexes as catalyst precursors in the oxidation of benzyl alcohol and ethylbenzene. Additionally, one of the complexes synthesized, $Cs[V^{V}O_2\{Hdfmp\text{-}(smdt)_2\}]$ **7**, was applied for the catalytic oxidation of (1) several primary and secondary alcohols to the corresponding aldehyde/ketone as well as of (2) several different simple arenes.

Experimental Section

Materials and methods

Acetyl acetone (Aldrich Chemicals Co., U.S.A), thiosemicarbazide, 30 % aqueous H_2O_2 (Rankem, India) and benzyl alcohol were used as supplied. Other chemicals and solvents were of analytical reagent grade. $[V^{IV}O(acac)_2]$,[32] 2,6-diformyl-4-methylphenol,[33] *S*-benzyldithiocarbazate[34] and *S*-methyldithiocarbazate[35] were prepared according to the methods reported in the literature.

Instrumentation and Characterization Procedures

Elemental analyses of the compounds were carried out either on an Elementar model Vario-El-III or in a FISONS EA 1108 CHNS-O apparatus. IR spectra were recorded as KBr pellets either on a Nicolet NEXUS Aligent 1100 series or a JASCO FT/IR 4100FT-IR spectrometer. Electronic spectra were measured in methanol either with an UV-1601 PC or with a Perkin Elmer lambda 35 UV-Vis spectrophotometer. ^{1}H NMR spectra were obtained on a Bruker 500 MHz, ^{13}C and [51]V NMR spectra on a Bruker Avance III 400 MHz spectrometer with the common parameter settings. NMR spectra were usually recorded in MeOD-d_4, and chemical shift [51]V values (δ^V) are referenced relative to neat V^VOCl_3 as external standard. EPR spectra were recorded with a Bruker ESP 300E X-band spectrometer and the spin Hamiltonian parameters were obtained by simulation of the spectra with the computer program of Rockenbauer and Korecz.[36] Thermogravimetric analyses of the complexes were carried out under oxygen atmosphere using a TG Stanton Redcroft STA 780 instrument.

A Shimadzu 2010 plus gas-chromatograph fitted with a Rtx-1 capillary column (30 m × 0.25 mm × 0.25 μm) and a FID detector was used to analyze the reaction products and their quantifications were made on the basis of the relative peak area of the respective product and using the appropriate standards. The identity of the products was confirmed using a GC-MS model Perkin-Elmer, Clarus 500 and comparing the fragments of each product with the library available.

The HPLC experiments were done on a Jasco System using an 880-51 (2-line degasser), an 887-PU (Intelligent Prep. Pump) and an 870-UV (Intelligent UV/Vis detector) with software BorWin. The solutions were analyzed through a LiChrosphere 100 RP-18 (5 μm) column using a MeOH/H_2O= 65/35 eluent, with a flow rate of 0.9 mL/min and detection at λ= 300 nm.

Preparation of Ligands

H₃dfmp-(smdt)₂ (I) and H₃dfmp-(sbdt)₂ (II). The ligands H₃dfmp-(smdt)₂ (**I**) and H₃dfmp-(sbdt)₂ (**II**) were prepared by a common procedure; the preparation of H₃dfmp-(smdt)₂ is described here. A solution of 2,6-diformyl-4-methylphenol (1.64 g, 10 mmol) dissolved in methanol (30 mL) was added to a solution of *S*-methyldithiocarbazate (3.96 g, 20 mmol) dissolved in methanol (10 mL). The obtained reaction mixture was refluxed on a water bath for 4

h. During this period a yellow solid slowly separated out. The separated yellow solid of **I** was filtered, washed with methanol followed by petroleum ether and dried over silica gel under vacuum.

Data for H$_3$dfmp-(smdt)$_2$ (I). Yield: 3.49 g (93.8%). Anal. Calc. for C$_{13}$H$_{16}$N$_4$S$_4$O (372.6): C, 41.91; H, 4.33; N, 15.04; S, 34.43%. Found: C, 41.52; H, 4.16; N, 15.18; S, 34.26%. ESI-MS(-): 370.9 u (100%) (C$_{13}$H$_{15}$N$_4$S$_4$O, exact mass = 371.01 u), 371.88 (25%).

Data for H$_3$dfmp-(sbdt)$_2$ (II). Yield: 4.93 g (94.0 %). Anal. Calc. for C$_{25}$H$_{24}$N$_4$S$_4$O (524.7): C, 57.22; H, 4.61; N, 10.69; S, 24.44%. Found: C, 56.92; H, 4.56; N, 10.58; S, 24.36%.

H$_3$dfmp-(tsc)$_2$ (III). Ligand **III** was prepared from 2,6-diformyl-4-methylphenol (1.64 g, 10 mmol) and thiosemicarbazide (1.828 g, 20 mmol) by the method outlined for **I**. Yield: 2.99 g (96.3%). Anal. Calc. for C$_{11}$H$_{14}$N$_6$S$_2$O (310.4): C, 42.57; H, 4.55; N, 27.08; S, 20.66%. Found: C, 42.72; H, 4.46; N, 27.19; S, 20.56%.

H$_3$dfmp-(smdt)$_2$ (**I**)   H$_3$dfmp-(sbdt)$_2$ (**II**)   H$_3$dfmp-(tsc)$_2$ (**III**)
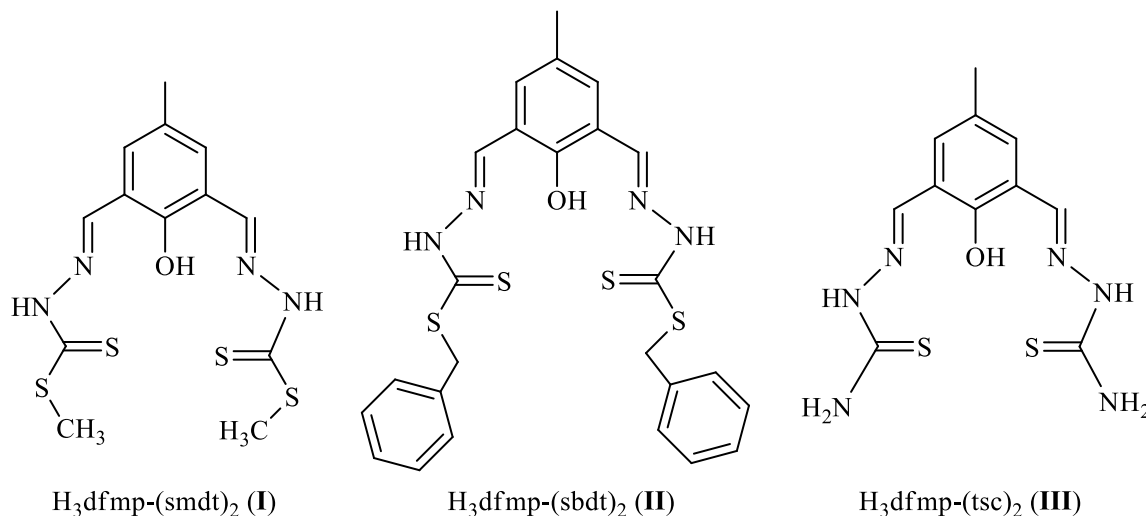
Fig. 1 Structural formulae of the ligand precursors described in this work.

Preparation of the vanadium Complexes

[V^{IV}O{Hdfmp-(smdt)$_2$}(CH$_3$OH)] (1). A solution of H$_3$dfmp-(smdt)$_2$ (0.372 g, 1 mmol) was prepared in absolute methanol (20 mL) by heating and filtered. A solution of [V^{IV}O(acac)$_2$] (0.265 g, 1 mmol) in methanol (15 mL) was added to the above solution with stirring; a

greenish-yellow solid started to precipitate immediately. After 4 h of stirring the solid was filtered, washed with methanol followed by petroleum ether (b.p. 60 ℃) and dried in a desiccator over silica gel. Yield: 3.76 g (80.2 %). Anal. Calc. for $C_{14}H_{19}N_4S_4O_3V$ (469.52): C 35.81; H 3.86; N 11.93; S 27.32 %. Found: C, 35.9; H, 3.9; N, 12.2; S 27.4 %. ESI-MS(-) 468.8 u (calc. $C_{14}H_{18}N_4O_3S_4V$ exact mass = 468.97 u).

[$V^{IV}O${Hdfmp-(sbdt)$_2$}(CH$_3$OH)] (2) and [$V^{IV}O${Hdfmp-(tsc)$_2$}(CH$_3$OH)] (3). Brown complexes **2** and **3** were prepared using H$_3$dfmp-(sbdt)$_2$ (**II**) and H$_3$dfmp-(tsc)$_2$ (**III**), respectively, and following the method outlined for **1**.

[$V^{IV}O${Hdfmp-(sbdt)$_2$}(CH$_3$OH)] (2). Yield: 0.491 g (80.1 %). Anal. Calc. for $C_{26}H_{25}N_4S_4O_3V$ (620.70): C, 50.31; H, 4.06; N, 9.03; S, 20.66%. Found: C, 50.4; H, 4.0; N, 8.9; S, 21.0%.

[$V^{IV}O${Hdfmp-(tsc)$_2$}(CH$_3$OH)] (3). Yield: 0.322 g (78.4 %). Colour: brown. Anal. Calc. for $C_{12}H_{15}N_6S_2O_3V$ (406.36): C, 35.47; H, 3.72; N, 20.68, S, 15.78%. Found: C, 35.9; H, 3.9; N, 20.8; S, 15.8%.

K[$V^{V}O_2${Hdfmp-(smdt)$_2$}] (4). A solution of KOH (0.112 g, 2 mmol) in methanol (15 mL) was added slowly to a solution of [$V^{IV}O${Hdfmp-(smdt)$_2$}(CH$_3$OH)] (0.469 g, 1 mmol) in methanol (150 mL) while stirring. The obtained orange solution was allowed to oxidize aerially at room temperature. After 2 days the color of the solution changed to yellow. After reducing the solvent volume to ca. 10 mL the mixture was kept for 12 h at room temperature. The separated yellow solid was filtered off, washed with methanol and dried in a desiccator over silica gel. Yield: 0.261 g (52.8 %). Anal. Calc. for $C_{13}H_{14}KN_4S_4O_3V$ (492.57): C, 31.70; H, 2.86; N, 11.37; S, 26.04%. Found: C, 31.17; H, 3.1; N, 11.2; S, 26.6%. ESI-MS(-): 452.8 u ($C_{13}H_{14}N_4O_3S_4V$ exact mass = 452.94).

K[$V^{V}O_2${Hdfmp-(sbdt)$_2$}] (5) and K[$V^{V}O_2${Hdfmp-(tsc)$_2$}] (6). Complexes **5** and **6** were prepared by the procedure outlined for **4**.

K[$V^{V}O_2${Hdfmp-(sbdt)$_2$}] (5). Yield: 0.373 g (58.4 %). Colour: yellow. Anal. Calc. for $C_{25}H_{24}N_4S_4O_3KV$ (644.8): C, 46.54; H, 3.44; N, 8.69; S, 19.89%. Found: C, 46.4; H, 3.0; N, 8.9; S, 20.2 %.

K[V^{V}O$_2$\{Hdfmp-(tsc)$_2$\}] (6). Yield: 0.219 g (51.4 %). Colour: yellow. Anal. Calc. for C$_{11}$H$_{11}$N$_6$S$_2$O$_3$KV (430.4): C, 30.70; H, 2.81; N, 19.53; S, 14.90%. Found: C, 30.4; H, 3.0; N, 19.0; S, 15.10%.

Cs[V^{V}O$_2$\{Hdfmp-(smdt)$_2$\}] (7). A solution of CsOH (0.330 g, 2 mmol) in methanol (15 mL) was added while stirring to a solution of [V^{IV}O\{Hdfmp-(smdt)$_2$\}(CH$_3$OH)] (0.469 g, 1 mmol) in methanol (150 mL) slowly. The obtained orange solution was left at room temperature for slow aerial oxidation. After 2 days the color of the solution slowly changed to yellow. After reducing the volume to ca. 10 mL the mixture was kept at room temperature for 12 h where yellow solid slowly separated out. This was filtered off, washed with methanol and dried in a desiccator over silica gel. Yield 0.351 g (61.01 %). Anal. Calc. for C$_{13}$H$_{14}$N$_4$S$_4$O$_3$CsV (586.38): C, 26.63; H, 2.41; N, 9.55; S, 21.87%. Found: C, 26.33; H, 2.57; N, 9.0; S, 22.3 %. ESI-MS(-): 453.0 (C$_{13}$H$_{14}$N$_4$O$_3$S$_4$V exact mass = 452.94).

Cs[V^{V}O$_2$\{(Hdfmp-(sbdt)$_2$\}] (8) and Cs[V^{V}O$_2$\{(Hdfmp-(tsc)$_2$\}] (9). These complexes were prepared similarly as mentioned for **6** using [V^{IV}O\{dfmp-(sbdt)$_2$\}(CH$_3$OH)] (**2**) and [V^{IV}O\{dfmp-(tsc)$_2$\}(CH$_3$OH)] (**3**), respectively.

Cs[V^{V}O$_2$\{(Hdfmp-(sbdt)$_2$\}] (8). Yield: 0.428 g (58.4 %). Colour: yellow. Anal. Calc. for C$_{25}$H$_{24}$N$_4$S$_4$O$_3$CsV (738.57): C, 40.66; H, 3.00; N, 7.59; S, 17.37%. Found: C, 40.4; H, 3.08; N, 6.9; S, 17.2%.

Cs[V^{V}O$_2$\{Hdfmp-(tsc)$_2$\}] (9). Yield: 0.431 g (68.4 %). Colour: brown. Anal. Calc. for C$_{11}$H$_{11}$N$_6$S$_2$O$_3$CsV (524.23): C, 25.20; H, 2.31; N, 16.03; S, 12.23%. Found: C, 25.5; H, 2.73; N, 15.9; S, 11.9%.

Catalytic oxidation of alcohols

The catalytic oxidation of benzyl alcohol, 4-isopropylbenzyl alcohol, 1-phenylethanol, cyclohexanol, isopropyl alcohol, 2-butanol and 3-methyl-1-butanol was carried out using a similar procedure using V^{V}O$_2$-complexes as catalyst precursors. Here experimental details are given for a representative substrate, benzyl alcohol, using Cs[V^{V}O$_2$\{Hdfmp-(smdt)$_2$\] (**7**). In a typical reaction, benzyl alcohol (1.08 g, 0.010 mol) and 30% aqueous H$_2$O$_2$ (2.3 g, 0.020 mol) were mixed in 5 mL of CH$_3$CN followed by addition of 0.002 g catalyst precursor. The reaction mixture was slowly stirred at 80 °C for 6 h. The obtained oxidation products, i.e. benzaldehyde,

benzoic acid and benzylbenzoate, were analyzed quantitatively using gas chromatography and by comparing their retention times with those of authentic samples; their identity was also confirmed by GC-MS. The catalytic reactions with the remaining substrates were carried out under the 'optimized' reaction conditions (details given in results and discussion section).

Catalytic oxidation of ethylbenzene

The catalytic oxidation of ethylbenzene was carried out in a 25 mL round bottom flask equipped with a magnetic stirrer and immersed in a thermostated oil bath. In a typical experiment, the catalyst precursor, a V^VO_2-complex (0.003 g) was added to ethylbenzene (1.08 g, 0.010 mol) and 30% aqueous H_2O_2((2.3 g, 0.020 mol) in CH_3CN (5 mL). The course of the reaction was monitored by GC-MS. The oxidation products were identified by comparing their retention times with those of authentic samples; their identity was also confirmed by GC-MS. Control reactions were carried out in the absence of catalyst, under the same conditions as the catalytic runs. No relevant amounts of products were detected.

Oxidation of other hydrocarbons e.g. tetraline, toluene, benzene and cumene was carried out similarly under the 'optimized' reaction conditions (details are given in results and discussion section).

Tests of sulfoxidation of ligand precursors

These tests were done with both H_3dfmp-(smdt)$_2$ (**I**) and $Cs[V^VO_2\{Hdfmp$-(smdt)$_2\}]$ (**7**) using a 10%, v/v, H_2O_2 solution (2.94 M), prepared by a dilution of a commercial 30% v/v solution with methanol (MeOH).

In a vial 1.1 mg (2.95×10^{-6} mol) of (**I**) in 2 mL of a 30% MeOH in acetonitrile solution, followed by the addition of 8 μL of the oxidant solution (2.35×10^{-5} mol). The mixture was left to stir at 60 °C and an HPLC of a 1:5 dilution of 100 μL in MeOH was performed every 2 h to follow the reaction up to 6 h. In another vial 2.15 mg (3.67×10^{-6} mol) of the complex were dissolved in 5 mL of CH_3CN followed by the addition of 15 μL of the H_2O_2 solution (4.41×10^{-5} mol). The mixture was left to stir at 60°C and an HPLC of a 1:2.5 dilution of 200 μL in MeOH was carried out every 2 h to follow the reaction up to 6 h.

The HPLC were performed on a Jasco System using an 880-51 (2-line degasser), an 887-PU (Intelligent Prep. Pump) and an 870-UV (Intelligent UV/Vis detector) with software BorWin. The solutions were analyzed through a LiChrosphere 100 RP-18 (5 μm) column using a MeOH/H$_2$O= 65/35 eluent; flow rate: 0.9 mL/min; detecting at λ= 300 nm. In the chromatograms the H$_3$dfmp-(smdt)$_2$ corresponds to a broad peak at ~13±3 min. The samples corresponding to the peaks that showed up were analyzed by ESI-MS (positive and negative modes.

Results and Discussion

[V^{IV}O(acac)$_2$] reacts with the ligand precursors H$_3$dfmp-(smdt)$_2$ (**I**), H$_3$dfmp-(sbdt)$_2$ (**II**) and H$_3$dfmp-(tsc)$_2$ (**III**) in 2:1 molar ratios in refluxing methanol to give the oxidovanadium(IV) (V^{IV}O) complexes [V^{IV}O{Hdfmp-(smdt)$_2$}(CH$_3$OH)] (**1**), [V^{IV}O{Hdfmp-(sbdt)$_2$}(CH$_3$OH)] (**2**) and [V^{IV}O{Hdfmp-(tsc)$_2$}(CH$_3$OH)] (**3**), respectively. Oxidation of these compounds in the presence of KOH gave the corresponding V^{V}O$_2$-species K[V^{V}O$_2${Hdfmp-(smdt)$_2$}] (**4**), K[V^{V}O$_2${Hdfmp-(sbdt)$_2$}] (**5**) and K[V^{V}O$_2${Hdfmp-(tsc)$_2$}] (**6**), or in presence of CsOH gave Cs[V^{V}O$_2${Hdfmp-(smdt)$_2$}] (**7**), Cs[V^{V}O$_2${Hdfmp-(sbdt)$_2$}] (**8**) and Cs[V^{V}O$_2${Hdfmp-(tsc)$_2$}] (**9**). Eqns. (1) to (3) summarize the synthetic procedures considering H$_3$dfmp-(smdt)$_2$ (**I**) as a representative ligand.

$$[V^{IV}O(acac)_2] + H_3dfmp\text{-}(smdt)_2 + CH_3OH \rightarrow [V^{IV}O\{Hdfmp\text{-}(smdt)_2\}(CH_3OH)] + 2Hacac \qquad (1)$$

$$[V^{IV}O\{Hdfmp\text{-}(smdt)_2\}(CH_3OH)] + 2KOH + \tfrac{1}{2}O_2 \rightarrow K[V^VO_2\{Hdfmp\text{-}(smdt)_2\}] + CH_3OH \qquad (2)$$

$$[V^{IV}O\{dfmp\text{-}(smdt)_2\}(CH_3OH)] + 2CsOH + \tfrac{1}{2}O_2 \rightarrow Cs[V^VO_2\{dfmp\text{-}(smdt)_2\}] + CH_3OH \qquad (3)$$
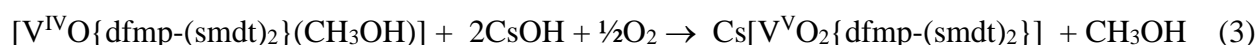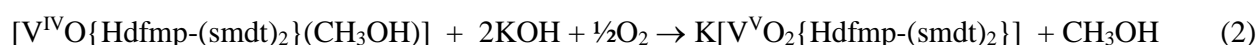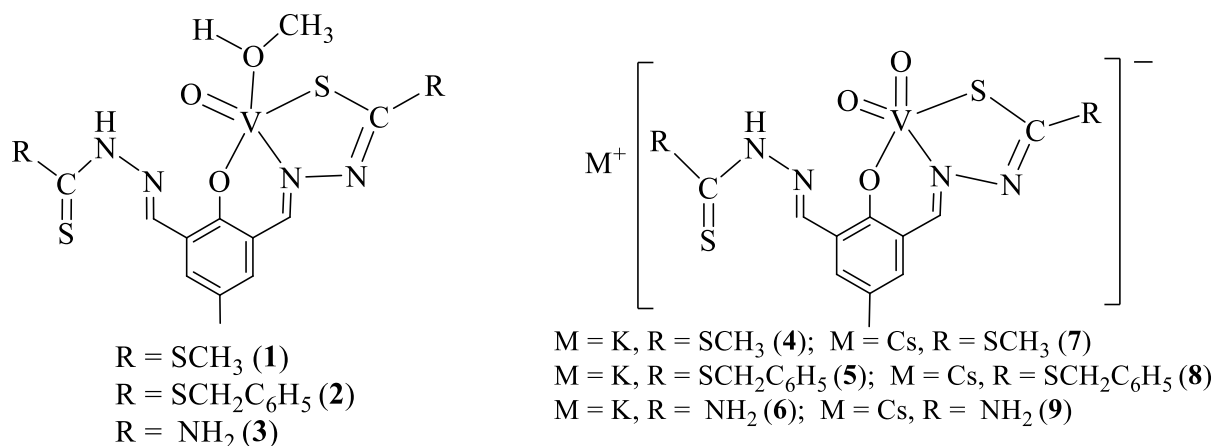
Fig. 2 provides an overview of the complexes described in this work. The structural formulae of each of these complexes is based on elemental analyses and spectroscopic (IR, UV-vis, EPR, ^{1}H, ^{13}C and ^{51}V NMR) data.

R = SCH$_3$ (**1**)
R = SCH$_2$C$_6$H$_5$ (**2**)
R = NH$_2$ (**3**)

M = K, R = SCH$_3$ (**4**); M = Cs, R = SCH$_3$ (**7**)
M = K, R = SCH$_2$C$_6$H$_5$ (**5**); M = Cs, R = SCH$_2$C$_6$H$_5$ (**8**)
M = K, R = NH$_2$ (**6**); M = Cs, R = NH$_2$ (**9**)

Fig. 2 Proposed structural formulae of V^{IV}O- and V^{V}O$_2$-complexes described in this work.

Thermal analysis

Thermal behavior of complexes **1-9** was studied under an oxygen atmosphere. The samples of **1-3** lose mass above 105 °C roughly corresponding to one solvent molecule, indicating the presence of weekly bound or adsorbed MeOH. Upon further increasing the temperature the solvent free complexes **1-3** decompose exothermically in one step with the formation of a residue of V$_2$O$_5$, while **4-9** decompose in two/ three overlapping steps forming MVO$_3$ (M = K or Cs) as final residues. The final weight of each residue agrees with that expected form the initial amount of complexes used (see Table ESI-1).
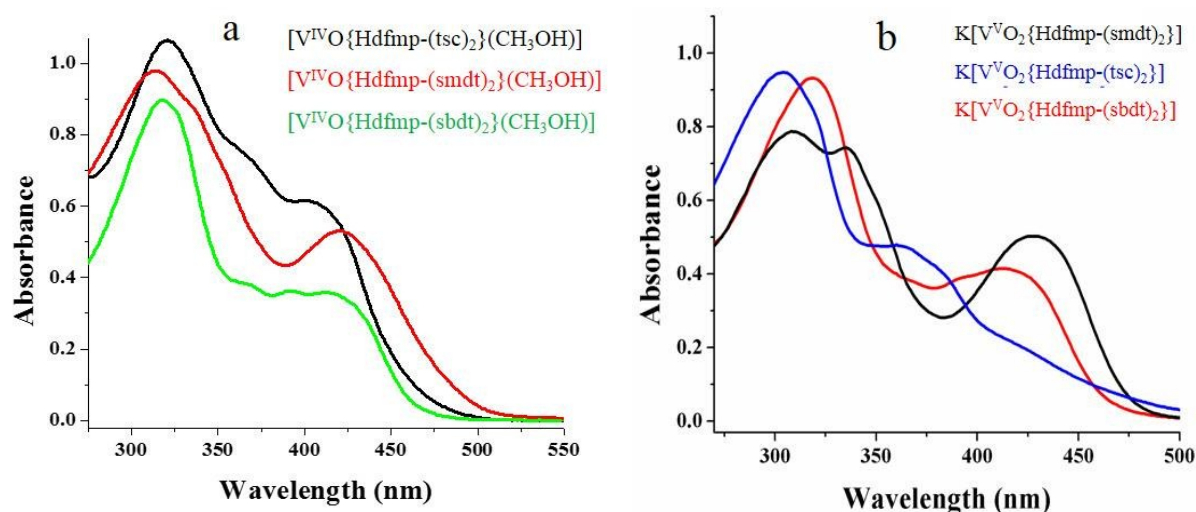
IR spectral study

Selected IR spectral data of the compounds are presented in Table ESI-2. The IR spectra of the ligands exhibit ν(N-H) and ν(C=S) at 2980–3098 cm^{-1} and 1023–1038 cm^{-1}, respectively. All complexes retain these two bands with some deviations along with the appearance of a new band in the region 1230-1280 cm^{-1}. The later one suggests the thioenolization of one of the S-containing moieties and replacement of H by the metal ion, while presence of former bands suggests that the ligands have at least one non-metal bound thionic group. Similarly, the ν(C=N) (azomethine) stretch, appearing at 1609 – 1616 cm^{-1} in ligands, splits into two: one remains at nearly the same position to that of respective ligand, while the other one shows up at lower wave number (1554-1560 cm^{-1}). This is also in the line of the coordination of N-atom of only one azomethine group.

The $V^{IV}O$-complexes exhibit a sharp band at 991-998 cm^{-1} due to ν(V=O) stretch[37] while $V^{V}O_2$-complexes exhibit two such sharp bands in the 908 – 921 and 890–897 cm^{-1} region assigned to ν_{asym}(O=V=O) and ν_{sym}(O=V=O) modes, respectively, typical of cis-$V^{V}O_2$-complexes.[38]

Electronic spectral study

Compounds H_3dfmp-(smdt)$_2$, H_3dfmp-(sbdt)$_2$ and H_3dfmp-(tsc)$_2$ exhibit absorption bands at ca. 206, 255, 328 and 360 nm which are assigned to $\varphi \to \varphi^*$, $\pi \to \pi_1^*$, $\pi \to \pi_2^*$, and n $\to\pi^*$ transitions, respectively. Similar slightly shifted bands are also observed in the corresponding complexes (Table ESI-3). In addition, new bands of medium intensity appear at ca. 410-450 nm, which is assigned to ligand to metal charge transfer (LMCT) bands (Fig. 3).

Upon dissolution the $V^{IV}O$-complexes have tendency to hydrolyze and oxidize (vide infra). Three bands at 751, 740 and 760 nm are observed at higher concentration of complexes **1**, **2** and **3**, respectively, which are assigned to d–d transitions. However, it is probable that these bands might be due to the presence of more than one isomer of each $V^{IV}O$-complex in solution. For the $V^{V}O_2$-complexes no such bands were detected.

Fig. 3 (a) UV-Vis spectra of the $V^{IV}O$-complexes in DMSO (each ca. 2.5±0.2×10^{-4} M. (b) UV-vis spectra of the $V^{V}O_2$-complexes in MeOH **4** (2.6×10^{-4} M), **5** (1.9×10^{-4} M) and **6** (2.8×10^{-4} M).
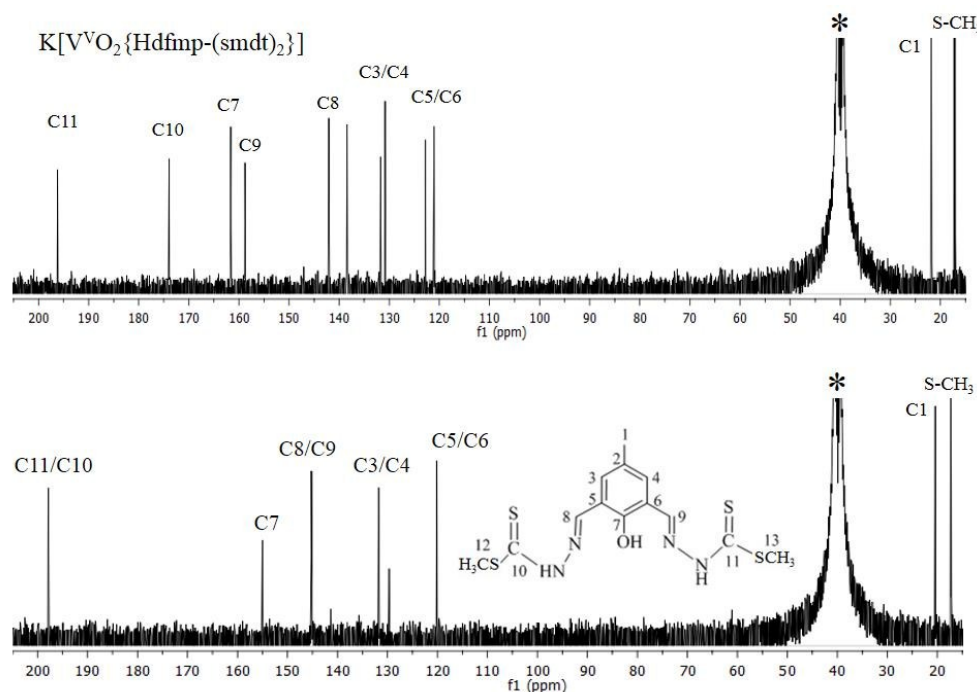
^{1}H NMR spectral study

The ^{1}H NMR spectra of the ligands and complexes were recorded to confirm their structure as well as coordinating modes of the ligands. The relevant spectral data are collected in Table 1. The broad signal appearing at δ = 9.56-10.90 ppm in the ligands due to the phenolic OH group is not seen in the spectra of the complexes, suggesting the coordination of the phenolate O-atom to the metal (Fig. ESI-1). The appearance of a new resonance significantly down field, equivalent to one proton in the complexes along with the original signal of the ligands equivalent to one proton due to the azomethine moiety demonstrates the coordination of the only one of the azomethine N-atom to the metal. Similarly, the resonance due to the hydrogen of -NH protons (equivalent to two protons) remains at nearly same position (but corresponding to only one proton) supports the enolization of only one of the NH groups and consequent replacement of H by the metal ion. Aromatic protons appear in the expected regions in spectra of the ligands and complexes with slight shifts in their positions. Signals due to the protons of the methyl appear well within the expected range.

Table 1 ^{1}H NMR spectral data of ligand precursors and V^VO_2-complexes in DMSO–d_6

Compounds	–CH=N–	Aromatic H	-OH	–NH	-CH$_3$	-NH$_2$
I	8.50 (d, 2H)	7.70 (s, 1H), 7.78 (s, 1H)	10.85 (s, H)	13.50 (s, 2H)	2.49 (s,3H), 2.5 (s,6H)	
4	8.86 (s, 1H) 8.84 (s, 1H)	7.73 (s,1H), 7.76 (s, 1H)		13.40 (s, 1H)	2.41 (s, 3H), 2.6 (s, 3H), 2.65 (s ,3H)	
7	8.86 (s, 1H) 8.84 (s, 1H)	7.73 (s,1H), 7.76 (s, 1H)		13.40 (s, 1H)	2.41 (s, 3H), 2.6 (s, 3H), 2.65 (s ,3H)	
II	8.50 (d, 2H)	7.57 (s, 5H), 7.51 (s, 5H) 7.70 (s, 1H), 7.78 (s,1H)	10.7 (s, 1H)	13. 35 (s, 2H)	2.4 (s,3H), 2.7 (m, 6H)	
5	8.81 (s,1H) 8.85 (s,1H)	7.51 (s, 5H), 7.6 (s, 5H) 7.70 (s, 1H), 7.78 (s,1H)		12.8 (s, 1H)	4.65 (s, 2H), 4.74(s, 2H), 2.4 (s, 3H)	
8	8.81 (s, 1H) 8.85 (s,1H)	7.51 (s, 5H), 7.6 (s, 5H), 7.70 (s, 1H), 7.78 (s,1H)		12.8 (s, 1H)	4.65 (s, 2H), 4.74 (s, 2H), 2.4 (s, 3H)	
III	8.36 (d, 2H)	7.64 (s, 1H), 7.59 (s, 1H)	9.56 (s, 1H)	11.52, 11.46	2.25 (s, 3H)	8.18, 8.08
6	8.45 (s, 1H) 8.52 (s,1H)	7.65 (s, 1H), 7.49 (s, 1H)		11.7 (s, 1H)	2.45 (s, 3H)	8.29 (s, 2H) 8.08 (s, 2H)
9	8.45 (s, 1H) 8.52 (s,1H	7.65 (s, 1H), 7.49 (s, 1H)		11.7 (s, 1H)	2.45 (s, 3H)	8.29 (s, 2H) 8.08 (s, 2H)

^{13}C NMR spectral study

The ^{13}C NMR spectra of the ligands are recorded (Table ESI-4) and the peaks are assigned based on the intensity patterns of the chemical shift and on the coordination-induced shifts ($\Delta\delta$) of the signals for carbon atoms in the vicinity of the coordinating atoms. These assignments also provide the useful information for the elucidation of the structures of the ligands and complexes. Compounds **I**, **II** and **III** display a lower number of resonances that the corresponding number of carbon atoms. This happened due to the presence of a centre of symmetry in the ligands. For example, complex K[V^{V}O$_2${Hdfmp-(smdt)$_2$}] (**4**) (Fig. 4), **s**hows 13 signals corresponding to the 13 carbon atoms present in the system.

Fig. 4 ^{13}C NMR spectra of H$_3$dfmp-(smdt)$_2$ (**I**) and of K[V^{V}O$_2${Hdfmp-(smdt)$_2$}] (**4**) recorded in DMSO–d$_6$. The (*) in figure indicates signal due to DMSO itself.

EPR study

The EPR spectra of "frozen" solutions (77 K) in DMSO of compounds **1 – 3** are depicted in (Fig. 5). The lines show broadening due to both incomplete rotational averaging of the g and A

tensors and probable partial precipitation of the complexes upon freezing the solutions. The spectra were simulated and the spin Hamiltonian parameters obtained by simulation of the spectra are included in Table 2.

The values of $|A_z|$ can be estimated using the additivity relationship [$A_z^{est} = \Sigma A_{z,i}$ (i = to 4)], ($A_{z,i}$ = contribution of each of the four donor atoms coordinated equatorially), proposed by Wüthrich and Chasteen with estimated accuracy of $\pm 3 \times 10^{-4}$ cm^{-1}. The $|A_z|$ values obtained for **1** – **3** (Table 2) agree with the $|A_z^{est}|$ values calculated from the partial contributions of the equatorial donor groups[20, 39-42] relevant in the present case {$O_{phenolate}$ (38.9×10^{-4} cm^{-1}), N_{imine} (38.1 to 43.7×10^{-4} cm^{-1}), O_{DMSO} (41.9×10^{-4} cm^{-1}), $S_{thiolate}$ (31.9×10^{-4} cm^{-1}), H_2O (45.7×10^{-4} cm^{-1})} either assuming a NSO_2 (species I) with H_2O coordination, or a NSO_2 (species II) with DMSO coordination, as equatorial binding sets. In both cases $S_{thiolate}$ is considered as an equatorial donor atom.[43]

Table 2 Spin Hamiltonian parameters obtained by simulation of the experimental 1st derivative EPR spectra recorded for DMSO solutions of complexes **1** – **3** at 77 K.

Complexes in DMSO (4 mM)		g_z	$\|A_z\|$ ($\times 10^{-4}$ cm^{-1})	g_x , g_y	$\|A_x\|$, $\|A_y\|$ ($\times 10^{-4}$ cm^{-1})
[$V^{IV}O${Hdfmp-(smdt)$_2$}] (**1**)	Species I	1.951	167.5	1.978	47.1
	Species II	1.946	155.4	1.979	47.5
[$V^{IV}O${Hdfmp-(sbdt)$_2$}] (**2**)	Species I	1.951	159.3	1.976	44.3
	Species II	1.948	155.5	1.975	44.4
[$V^{IV}O${Hdfmp-(tsc)$_2$}] (**3**)	Species I	1.956	159.8	1.978	44.7
	Species II	1.942	156.8	1.975	44.6
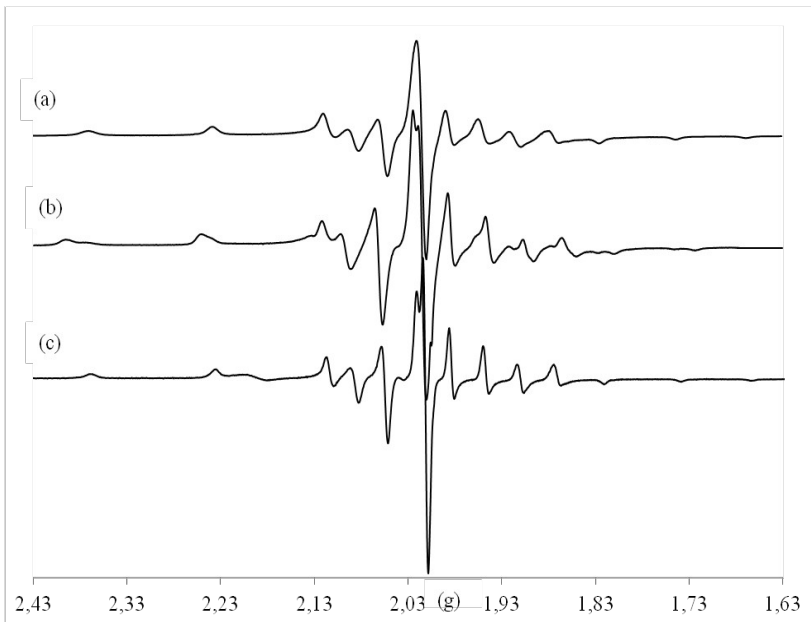
Fig. 5 First derivative EPR spectra of frozen (77 K) solutions (ca. 4 mM) (a) [V^{IV}O{Hdfmp-(sbdt)$_2$}] (**2**) (b) [V^{IV}O{Hdfmp-(smdt)$_2$}] (**1**) in DMSO and (c) [V^{IV}O{Hdfmp-(tsc)$_2$}] (**3**) in DMSO.

^{51}V NMR study

　　　The V^{V}O$_2$-complexes were further characterized in solution by recording their ^{51}V NMR spectra in DMSO-d$_6$. The ^{51}V chemical shift values (δ_V) are reported in Table 3. The resonances are somewhat broadened due to quadrupolar interactions; the line widths at half height are around 200 Hz, which may be considered comparatively narrow in ^{51}V NMR spectroscopy.[42,44,45] Complexes **4 – 9** display one strong resonance in the –450.0 to –468.5 ppm region, values in agreement with other reported examples where S-atoms participate in coordination in addition to the O and N donor atoms.[42,46]

Table 3 Summary of the ^{51}V NMR data (δ_V values) of the V^{V}O$_2$-complexes studied in this work in DMSO-d$_6$.

Compounds	Chemical shifts (δ_V/ppm)	Compounds	Chemical shifts (δ_V/ppm)
K[V^{V}O$_2${Hdfmp-(smdt)$_2$}] (**4**)	–464.1	Cs[V^{V}O$_2${Hdfmp-(smdt)$_2$}] (**7**)	–464.0
K[V^{V}O$_2${Hdfmp-(sbdt)$_2$}] (**5**)	–464.3	Cs[V^{V}O$_2${Hdfmp-(sbdt)$_2$}] (**8**)	–459.8
K[V^{V}O$_2${Hdfmp-(tsc)$_2$}] (**6**)	–450.0	Cs[V^{V}O$_2${Hdfmp-(tsc)$_2$}] (**9**)	–460.9

Several experiments were carried out to detect the possible formation of V^V-species in solutions containing Hdfmp-(smdt)$_2$ (**I**) and V^VO_2-complexes. Fig. ESI-2 depicts ^{51}V NMR spectra of a solution of [$V^{IV}O${Hdfmp-(smdt)$_2$}(MeOH)] (**1**) in MeOD a few minutes after addition of KOH, and with time up to 72 h. Initially a resonance at ca. -405 ppm is detected; after 2 h and till 72 h, only the resonance with $\delta_V = -453$ ppm, corresponding to the formation of [V^VO_2{Hdfmp-(smdt)$_2$}]$^-$ is detected. In similar experiments but adding CsOH in MeOD, instead of KOH, Fig. 6, only the resonance with $\delta_V = -453$ ppm was detected.
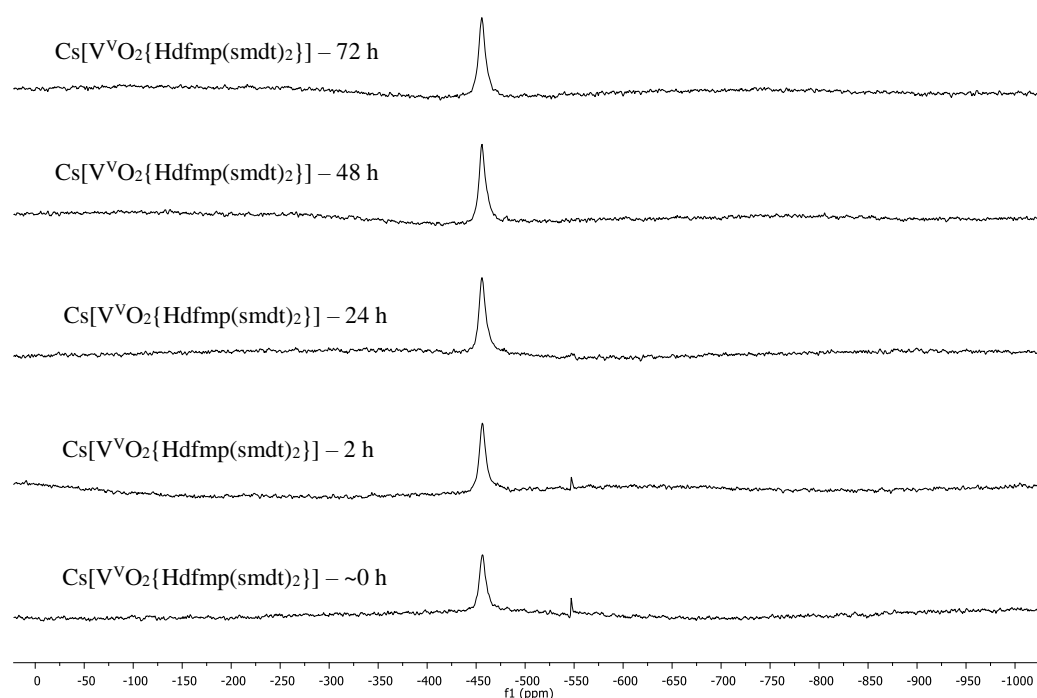
Fig. 6 ^{51}V NMR spectra of solutions of Cs[V^VO_2{Hdfmp-(smdt)$_2$}] (**7**) in MeOD. The spectra were measured upon addition of a solution of CsOH in MeOD, and after 2, 24, 48 and 72 h, to [$V^{IV}O${Hdfmp(smdt)$_2$}(MeOH)] (**1**) (4 mM) in MeOD.

Experiments were also carried out to detect the possible formation of [$V^VO(O_2)$(Hdfmp-(smdt)$_2$] species in solutions containing either **4** or **7** in MeOD upon additions of an aqueous solution of H$_2$O$_2$. In these solutions only the resonances corresponding to [V^VO_2{Hdfmp-(smdt)$_2$}]$^-$ were detected, even upon addition of relatively high excesses of H$_2$O$_2$. Upon addition

16

of an excess of H_2O_2, and observation of the resonance at -453 ppm, after ca. 24 h these peaks either disappeared (case of **4**) (Fig. ESI-3), or decreased significantly its intensity (case of **7**) (Fig. ESI-4). Thus, after 24 h either the V^V was reduced to a V^{IV}-containing species or some type of not clearly visible solid formed, not allowing obtaining the ^{51}V NMR resonances. Globally, if any V^VO-(O$_2$)-dfmp-(smdt)$_2$} species form in solution, they could not be detected in these ^{51}V NMR measurements.

Experiments were also carried out adding *tert*-butylhydroperoxide (*t*-BuOOH) to solutions of Cs[V^VO_2{Hdfmp-(smdt)$_2$}] in 10% CD$_3$OD:CH$_3$OH (Fig ESI-5A). Also in this case only the resonance at -453 ppm was detected, at least up to a molar ratio *t*-BuOOH:**7** of 10. Therefore, if any V^VO-(t-BuOOH)-dfmp-(smdt)$_2$} species form in solution, they could not be detected in these ^{51}V NMR measurements.

Assays were also carried out adding HCl to solutions of Cs[V^VO_2{Hdfmp-(smdt)$_2$}] in MeOH (Fig ESI-5B). Up to a ratio of added HCl : **7** of 3:1, only the resonance at -453 ppm was detected. For the ratios 5:1 and 10:1, the solution turned yellow and only a resonance at -402 ppm was recorded, this probably being due to the formation of [$V^VO(OH)${Hdfmp-(smdt)$_2$}] at lower pH values. Similar observations of resonances at downfield δ_V values upon addition of acid have been reported and were also explained as due to the formation of oxidohydroxidovanadium(IV) complexes.[27, 47-50]

Reactivity of complexes

Reactivity of oxidovanadium(IV) and dioxidovanadium(V) complexes with H_2O_2

The oxidovanadium(IV) complexes, [$V^{IV}O${Hdfmp-(smdt)$_2$}(CH$_3$OH)]] (**1**), [$V^{IV}O${Hdfmp-(sbdt)$_2$}(CH$_3$OH)]] (**2**) and [$V^{IV}O${Hdfmp-(tsc)$_2$}(CH$_3$OH)]] (**3**) in DMSO depict changes upon addition of H_2O_2 which were monitored by electronic absorption spectroscopy. The changes observed in the case of [$V^{IV}O${Hdfmp-(smdt)$_2$(CH$_3$OH)}]] are depicted in Fig. 7. The progressive addition of a dilute solution of H_2O_2 in DMSO, prepared by adding the required amount of a 30% aqueous H_2O_2, to a solution of [$V^{IV}O${Hdfmp-(smdt)$_2$}]] in DMSO resulted in the flattening of the d-d band (at ca. 751 nm). Disappearance of this band indicates the oxidation of the vanadium(IV) center to a higher oxidation state. The intensity of charge transfer band at 422 nm decreased and finally disappeared.
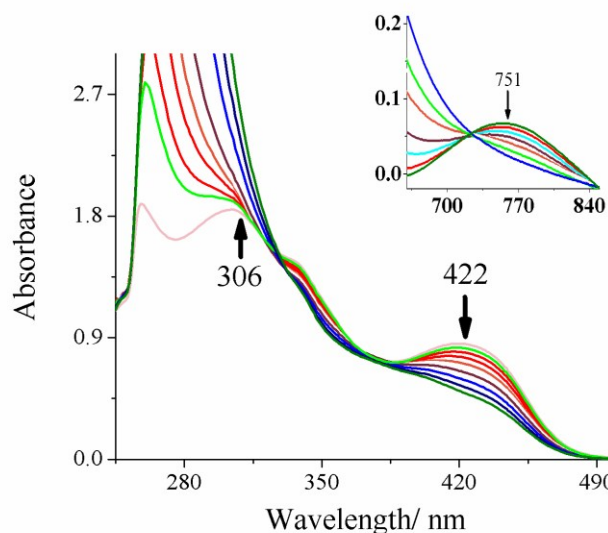
Fig. 7 Titration of 25 mL of a 5.3×10^{-4} M solution of [$V^{IV}O${Hdfmp-(smdt)$_2$(CH$_3$OH)}] (**1**) in DMSO with H$_2$O$_2$. The UV-Vis absorption spectra were recorded upon stepwise additions of one drop portions of a H$_2$O$_2$ solution (2.3×10^{-2} M in DMSO), prepared by adding the required amount of a 30% aqueous H$_2$O$_2$. The inset shows an expanded spectral region (700 – 840 nm); these spectra were recorded upon stepwise additions of one drop portions of a H$_2$O$_2$ solution (4.2×10^{-2} M in DMSO) to 25 mL of a 4.5×10^{-3} M solution in DMSO.

Complex [$V^{IV}O${Hdfmp-(sbdt)$_2$(CH$_3$OH)}] depicted different trends. Here, the charge transfer band appearing at ~413 nm slowly shifts to ~425 nm without changing its intensity. Bands of other regions remain in nearly the same positions as in the original complex (Fig. 8). Notwithstanding, the progressive addition of a dilute H$_2$O$_2$ solution in DMSO to a solution of [$V^{IV}O_2${Hdfmp-(sbdt)$_2$}] in DMSO resulted in the flattening of the d – d band (at ca. 740 nm), showing that the V^{IV}-center oxidizes to V^V upon addition of H$_2$O$_2$.
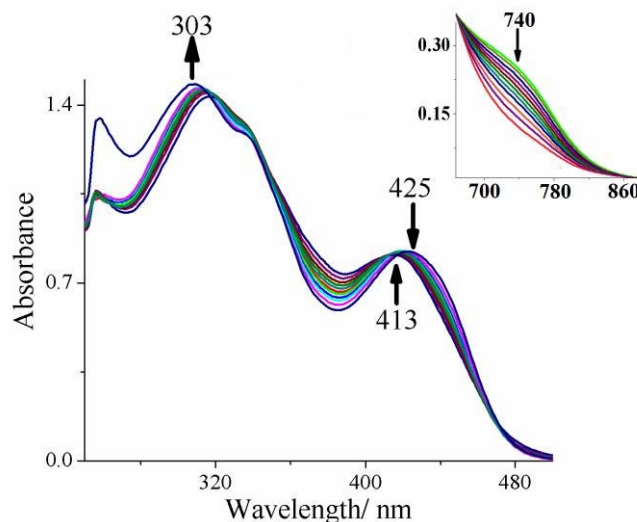
Fig. 8 Titration of 25 mL of a 8.3×10^{-4} M solution in DMSO of [V^{IV}O{Hdfmp-(sbdt)$_2$(CH$_3$OH)}] (**2**) with H$_2$O$_2$. The UV-Vis spectra were recorded upon stepwise additions of one drop portions of a H$_2$O$_2$ solution (2.1×10^{-2} M in DMSO). The inset shows the expanded spectral region (700 – 850 nm); these were recorded upon stepwise additions of one drop portions of a H$_2$O$_2$ solution (3.8×10^{-2} M in DMSO), also prepared by adding the required amount of a 30% aqueous H$_2$O$_2$, to 25 mL of a 7.2×10^{-3} M solution of the complex in DMSO.

In the experiment with [V^{IV}O{Hdfmp-(smdt)$_2$(CH$_3$OH)}] (**1**), it is clear that upon adding H$_2$O$_2$ the process $V^{IV} \rightarrow V^{V}$ took place, but there is no obvious indication that a V^{V}O-O$_2$-{Hdfmp-(smdt)$_2$(CH$_3$OH)} species might have formed. The appearance of the shoulder band at ca. 340-350 nm, at some stage of addition of H$_2$O$_2$ might be an indication for the formation of the diperoxido complex V^{V}O(O$_2$)$_2$,[51] but not of V^{V}O(O$_2$) species. For higher amounts of H$_2$O$_2$ probably there are no more V^{V}O-Hdfmp-(smdt)$_2$ species in solution. In contrast, with [V^{IV}O{Hdfmp-(sbdt)$_2$(CH$_3$OH)}] (**2**), upon additions of H$_2$O$_2$ the appearance of the band at ca. 425 nm (and at ca. 310 nm) suggests the formation of V^{V}O-O$_2$-Hdfmp-(sbdt)$_2$ species.[52]

Upon additions of three drops of a dilute H$_2$O$_2$ solution in DMSO to a solution of [V^{IV}O{Hdfmp-(tsc)$_2$(CH$_3$OH)}] (**3**) in DMSO, the intensity of the charge transfer band appearing at ~428 nm slowly decreases along with the appearance of a weak shoulder at ca. 385 nm (Fig. ESI-6). Simultaneously, the 370 nm band gained intensity, while the 318 nm band increased its intensity along with slight shift to ~312 nm. The d-d band appearing at 760 nm

slowly flattened and finally almost disappeared. This experiment demonstrates that upon addition of H_2O_2, with time the V^{IV}-center oxidizes to V^V upon addition of H_2O_2. The maintenance of clear bands at ca. 370 and 312 nm[53] suggests that V^VO-O_2-dfmp(tsc)$_2$ species form in these conditions.

Adding a dilute H_2O_2 solution in DMSO to solutions of the V^VO_2-complexes, instead of the corresponding V^VO-compounds, some trends observed were somewhat different. In the case of Cs[V^VO_2{Hdfmp-(smdt)$_2$}] (**7**), the intensity of the charge transfer band at 421 nm slowly decreased and flattened, while a new band appeared at 375 nm. The intensity of the ~306 nm band decreased and finally almost disappeared (Fig. 9). This suggests that V^VO-O_2-dfmp(smdt)$_2$ species formed, with λ_{max} at ~375 and ~310 nm.[52]
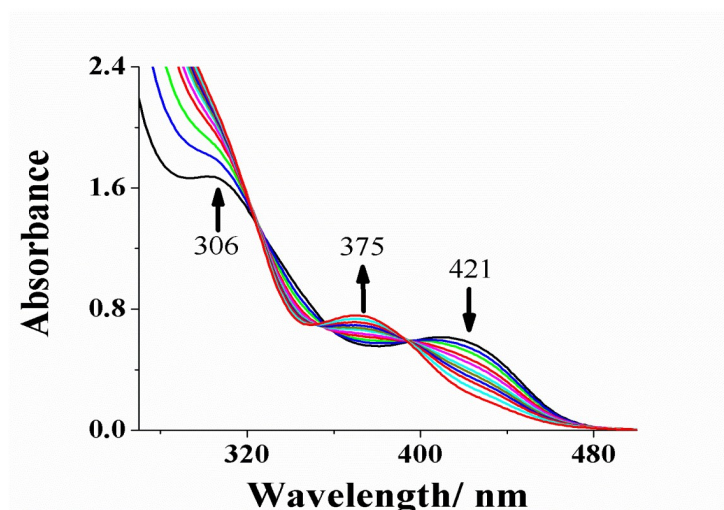
Fig. 9 Titration of 25 mL of a 4.3×10^{-4} M solution in CH_3OH of Cs[V^VO_2{Hdfmp-(smdt)$_2$}]. The absorption spectra were recorded upon stepwise additions of one drop portions of a H_2O_2 solution (2.2×10^{-2} M in DMSO, prepared by adding the required amount of a 30% aqueous H_2O_2).

In the experiments with both H_3dfmp-(smdt)$_2$ (**I**) and Cs[V^VO_2{Hdfmp-(smdt)$_2$}] (**7**) adding a ~10-fold excess of H_2O_2 solution leaving the mixtures stirring at 60 °C for 6 h, and controlling the evolution of the solutions by HPLC, extensive hydrolysis of the V^VO_2-complex was noticed, but no clear peaks corresponding to sulfoxidation products of **I** were obtained.

Complexes $Cs[V^VO_2\{Hdfmp\text{-}(sbdt)_2\}]$ (**8**) (Fig. ESI-7) and $Cs[V^VO_2\{Hdfmp\text{-}(tsc)_2\}]$ (**9**)) (Fig. ESI-8) exhibit rather similar trends upon additions of dilute H_2O_2 solutions. The intensity of CT bands appearing at ~423 nm (for **8**) and at 414 nm (for **9**) gradually decreases, and the band at ~364 nm shifts to 359 nm in the case of compound **8**, while the band at ~364 nm of **9** increases intensity upon the addition of the H_2O_2 solution. Again these trends, namely the observation of bands at these λ_{max} values suggest the formation of either $V^VO\text{-}O_2\text{-}dfmp(sbdt)_2$ or $V^VO\text{-}O_2\text{-}dfmp(tsc)_2$ species, as was reported for many other peroxidovanadate complexes.[52]

Reactivity of oxidovanadium(IV) complexes with HCl

The behavior of a methanolic solution of $[V^{IV}O\{Hdfmp\text{-}(smdt)_2(CH_3OH)\}]$ (**1**) upon addition of HCl was studied by drop wise addition of a methanolic solution of HCl to 25 mL of a solution of **1**. The changes observed are presented in Fig. 10(a). The intensity of band appearing at 433 nm decreased. Simultaneously, the weak band appearing at 401 nm sharpens with slight gain in intensity. The band at 256 nm loses its intensity while the band at ~325 nm shifts to ~349 nm with gain in intensity. In the case of $[V^{IV}O\{Hdfmp\text{-}(sbdt)_2(CH_3OH)\}]$ (**2**) the results are rather similar (Fig. 10(b)), the band at 414 nm disappears gradually. Simultaneously, band at 314 nm gains intensity shifting to ~329 nm. The solution became dark at the end the HCl additions. Such changes have been interpreted as partial hydrolysis of the complexes, oxidation of V(IV) to V(V) and formation of oxidohydroxidovanadium(V) species. The formation of $V^VO(OH)L$ complexes upon addition of acid has been previously reported.[18,19,47,48,53] The experiments with the other complexes yielded similar results.
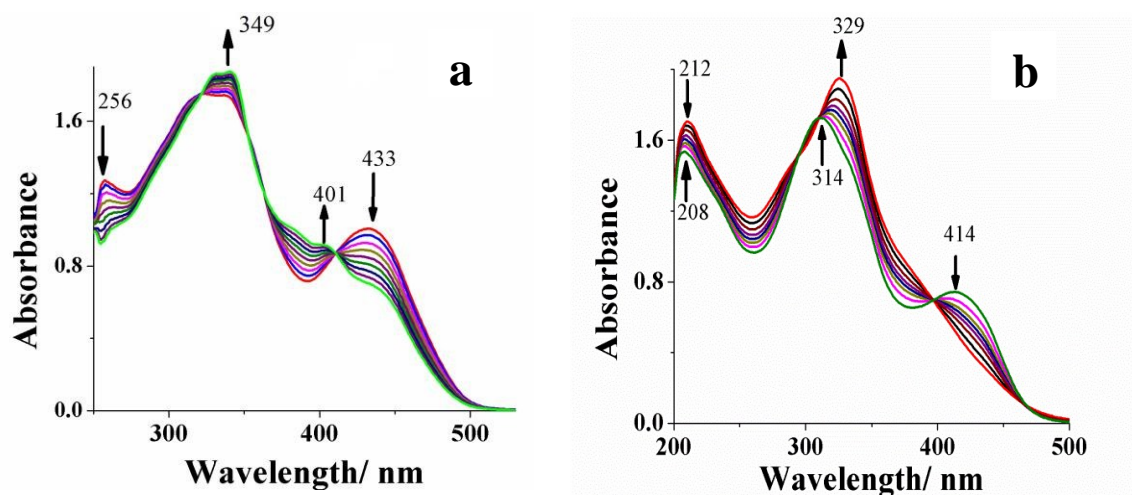
Fig. 10 (a) Titration of methanolic solution of $[V^{IV}O\{Hdfmp\text{-}(smdt)_2(CH_3OH)\}]$ (**1**) with HCl solution. The spectra were recorded upon stepwise addition of two drop portions of HCl solution (prepared by dissolving two drops of 12.5 M HCl in 10 mL of MeOH) to 25 mL of 2.3×10^{-4} M solution of (**1**) in CH_3OH. (b) Titration of methanolic solution of $[V^{IV}O\{Hdfmp\text{-}(sbdt)_2(CH_3OH)\}]$ (**2**) with HCl solution. The spectra were recorded upon stepwise addition of two drop portions of HCl solution (prepared by dissolving two drops of 12.5 M HCl in 10 mL of MeOH) to 25 mL of 3.4×10^{-4} M solution of **2** in CH_3OH.

Catalytic oxidations

Oxidation of benzyl alcohol

The oxidation of alcohols is one of the important reactions of organic molecules. These reactions may involve quite different terminal oxidants and metal catalysts are capable of promoting this reaction. Vanadium compounds have been used as catalyst precursors and the subject was recently reviewed.[23] We tested the efficacy of the presently synthesized complexes for the catalytic oxidation of primary and secondary alcohols using aqueous H_2O_2 as oxidant and taking benzyl alcohol as a reference compound to establish the best experimental conditions.

Generally, the oxidation of benzyl alcohol gives mainly three products: benzaldehyde, benzoic acid and benzyl benzoate, which were also observed previously.[54]

benzyl alcohol   benzaldehyde   benzoic acid   benzyl benzoate
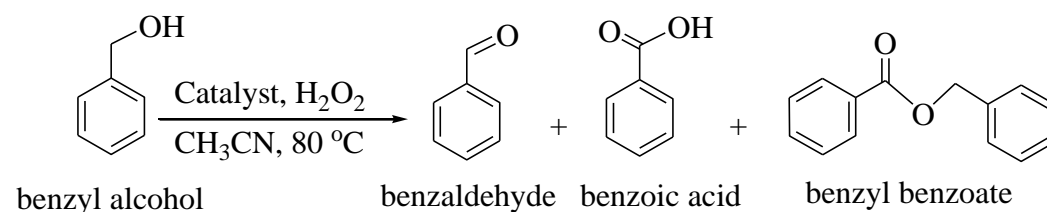
Scheme 1 Oxidation of benzyl alcohol catalyzed by oxidovanadium(V) complexes.

In order to achieve the maximum oxidation products of benzyl alcohol the effects of the following parameters were studied in detail using $Cs[V^VO_2\{Hdfmp\text{-}(smdt)_2\}]$ (**7**) as a representative catalyst:

i. Amount of catalyst

ii. Amount of H_2O_2

iii. Amount of solvent

iv. Temperature.

The effect of different amounts of catalyst in the oxidation of benzyl alcohol was checked. Three different amounts of catalyst were taken in the mixture of benzyl alcohol (1.08 g, 10 mmol), 30% H_2O_2 (2.27 g, 0.020 mmol) and 5 mL of acetonitrile and the reaction was carried out at 80 ℃. As shown in Fig. 11(a), increasing the amount of catalyst from 0.002 g to 0.003 g, the overall % conversion increases from 60 to 72 %. Upon further increase of the catalyst amount to 0.004 g, the overall conversion remained constant (73%). The order of the selectivity of products for 0.002 g of catalyst after 2 h of reaction was: benzaldehyde (89%) > benzyl benzoate (9%) > benzoic acid (1%). In the case of 0.003 g of catalyst, the selectivity of products followed the order: benzaldehyde (90%) > benzoic acid (6%)> benzyl benzoate (2%), whereas for 0.004 g of catalyst the selectivity order was: benzaldehyde (91%) > benzoic acid (6%) > benzyl benzoate (1%). Therefore, an amount of 0.003 g of catalyst was considered as optimum for optimizing the remaining conditions.

The effect of amount of oxidant (30% aqueous H_2O_2) for the oxidation of benzyl alcohol is illustrated in Fig. 11(b). Under above conditions, a oxidant:substrate ratio of 1:1 gave 48% conversion with 88% selectivity of benzaldehyde, 9% of benzoic acid and 2% of benzyl benzoate. Increasing this ratio to 2:1 improved the conversion to 90%, while conversion remained almost constant on further increasing this ratio to 3:1. With higher amounts of oxidant the conversion did not increase much possibly due to the presence of larger amounts of water. Therefore, a substrate:H_2O_2 ratio of 1:2 was considered suitable to optimize the other conditions.

Similarly, the effect of solvent was studied considering 5, 7 and 10 mL of acetonitrile. Under the above conditions, 5 mL acetonitrile gave 70% conversion with selectivity of benzaldehyde (90%), benzoic acid (7%) and benzyl benzoate (2%), while increasing the solvent volume to 7 mL did not improve the overall conversion of benzyl alcohol. Upon further increment of solvent to 10 mL the conversion remained almost same (Fig. 11(c)). Therefore, 5 mL was considered as optimized under these reaction conditions.

Under the optimized reaction conditions i.e. benzyl alcohol (1.08 g, 0.010 mol), catalyst (0.003 g), 30% H_2O_2 (2.27 g, 0.020 mol) and acetonitrile (5 mL), the reaction was carried out at three

23

different temperatures: 60, 70 and 80 ºC. A maximum of 42% conversion was obtained at 60 ºC. This conversion improved to 60% at 70 ºC and to 73% at 80 ºC (Fig. 11(d)). Therefore, we chose 80 ℃ as the optimized reaction temperature. Table ESI-5 summarizes some of the data of the above described experiments.
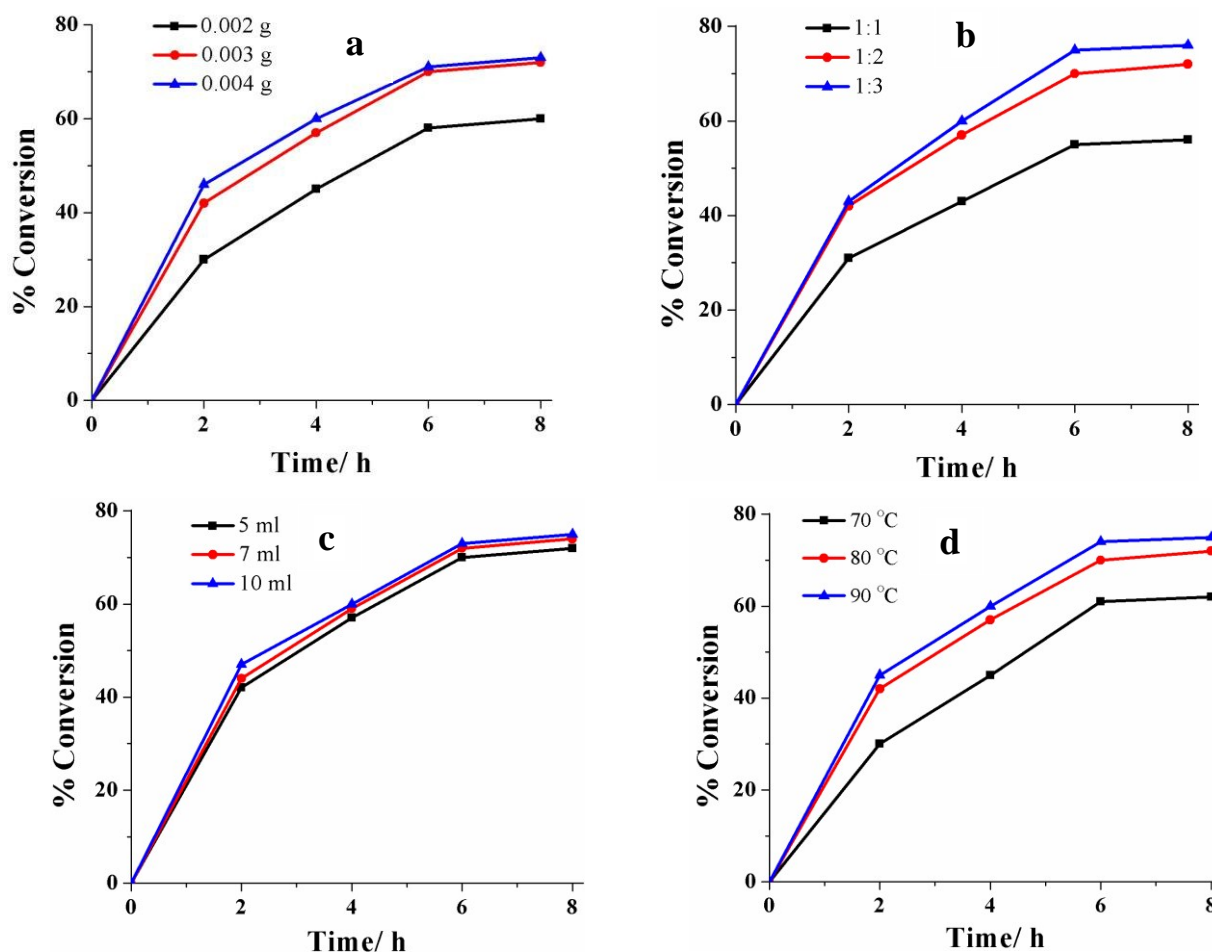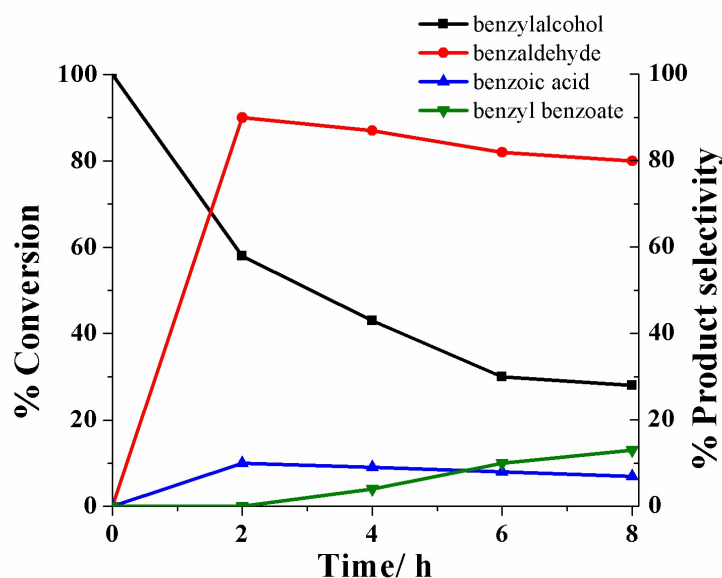

Fig. 11 Catalytic oxidation of benzyl alcohol using $Cs[V^VO_2\{Hdfmp\text{-}(smdt)_2\}]$ (**7**) as catalyst precursor. (a) Effect of different amounts of catalyst precursor; other reaction conditions: benzyl alcohol (1.08 g, 10 mmol), 30% H_2O_2 (2.27 g, 0.020 mol), acetonitrile (5 mL) and reaction temp. 80 ºC. (b) Effect of different substrate:oxidant ratios; other reaction conditions: benzyl alcohol (1.08 g, 0.010 mol), catalyst (0.003 g), acetonitrile (5 mL) and reaction temp. 80 ºC. (c) Effect of amount of solvent (acetonitrile); other reaction conditions: benzyl alcohol (1.08 g, 0.010 mol), catalyst (0.003 g), 30% H_2O_2 (2.27 g, 0.020 mol) and reaction temp. 80 ºC. (d) Effect of

temperature; other reaction conditions: benzyl alcohol (1.08 g, 0.010 mol), catalyst precursor (0.003 g), 30% H_2O_2 (2.27 g, 0.020 mol) and acetonitrile (5 mL).

Under the above optimized reaction conditions a blank reaction was carried out without addition of catalyst which yielded the percent conversion of only 6% (Fig. ESI-9).

Table ESI-5 presents oxidation of benzyl alcohol under different reactions. Taking the data from entry no 2, considered as the best suited for the reaction, where 72% conversion of benzyl alcohol is achieved. The formation of three products starts with the consumption of benzyl alcohol (Fig. 12). The selectivity for the formation of benzaldehyde is by far the highest amongst all products. After 2 h of the reaction the selectivity of benzaldehyde reaches 90% and then decreases to 80% at the end of 8 h, possibly due to overoxidation: formation of small amounts of benzoic acid, which reaches 7% at the end of 8 h (Fig. 12). Part of the benzoic acid reacts with benzyl alcohol to give benzyl benzoate and its overall conversion reaches 13 %.

Fig. 12 Profile showing the % consumption of benzyl alcohol along with the % selectivity of the formation of products using $Cs[V^VO_2\{Hdfmp\text{-}(smdt)_2\}]$ (**7**) as catalyst precursor under the optimized reaction conditions (entry no 2 of Table ESI-5).
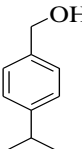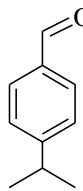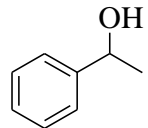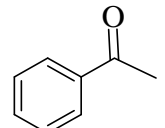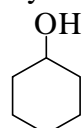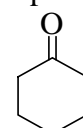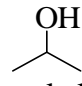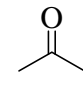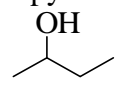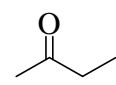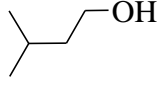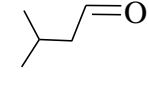
We also tested the catalytic potential of two other V^VO_2-complexes, $Cs[V^VO_2\{Hdfmp-(sbdt)_2\}]$ (**8**) and $Cs[V^VO_2\{Hdfmp-(tsc)_2\}]$ (**9**) for the oxidation of benzyl alcohol under the optimized reaction conditions mentioned above. Use of $Cs[V^VO_2\{Hdfmp-(sbdt)_2\}]$ gave 73% conversion while $Cs[V^VO\{Hdfmp-(tsc)_2\}]$ gave 70% conversion. Fig. ESI-10 compares conversion profiles of all three catalyst precursors under optimized reaction conditions and Table 4 presents turn over frequency and selectivity data of products for these catalysts. It is clear that there are not much differences between the performances of the three compounds.

Table 4 Conversion of benzyl alcohol, TOF and product selectivity. Conditions: benzyl alcohol (1.08 g, 0.010 mol), catalyst precursor (0.003 g), 30% aqueous H_2O_2 (2.27 g, 0.020 mol), acetonitrile (5 mL) and temperature 80 °C.

S. No.	Catalyst	Conv. (%)	TOF/ h^{-1}	Selectivity (%)		
				Benzaldehyde	Benzoic acid	Benzyl benzoate
1.	$Cs[V^VO_2\{Hdfmp-(smdt)_2\}]$	72	240	80	7	13
2	$Cs[V^VO_2\{Hdfmp-(sbdt)_2\}]$	73	304	78	4	15
2	$Cs[V^VO_2\{Hdfmp-(tsc)_2\}]$	70	206	80	5	14

Under the above reaction conditions, the oxidation of other primary and secondary alcohols was also tested. Table 5 presents the conversion of alcohols as well as the selectivity of the key product i.e., the corresponding aldehyde/ketone. Amongst the secondary alcohols studied 2-butanol gave maximum conversion of 95% followed by 1-phenylethanol with 90% conversion. Similarly amongst the primary alcohol tested, $Cs[V^VO_2\{Hdfmp-(smdt)_2\}]$ (**7**) showed the highest conversion of 82% for 3-methyl-1-butanol (isoamyl alcohol). The selectivity of the products was 100% in all cases except for 4-isopropylbenzyl alcohol, where the formation of a small amount 4-isoporpylbenzoic acid was also obtained.

26

Table 5 Conversion of several different alcohols to the corresponding aldehyde/ketone, their TOF and product selectivity using $Cs[V^VO_2\{Hdfmp\text{-}(smdt)_2\}]$ (**7**) as catalyst precursor.[a]

| Sr No	Substrate	Product	Conv. (%)	Product selectivity (%)	TOF/h^{-1}
1	4-isopropylbenzyl alcohol	4-isopropylbenzaldehyde	70	83	441
2	1-phenyl ethanol	acetophenone	90	100	662
3	cyclohexanol	cyclohexanone	25	100	17
4	isopropyl alcohol	acetone	75	100	536
5	2-butanol	2-butanone	95	100	679
6	3-methyl-1-butanol	3-methyl-1-butanal	82	100	586

[a] Reaction conditions: substrate (0.010 mol), catalyst (0.003 g), 30% aqueous H_2O_2 (2.27 g, 0.020 mol), acetonitrile (5 mL) and temperature 80 °C.

Oxidation of arenes

The oxidation of simple arenes is an important type of transformation in fine chemicals industry. For example, phenol is an important molecular precursor of many high value aromatics and resins. Thus the direct and selective oxidation of benzene and several other aromatic compounds are reactions that require suitable catalytic processes. Vanadium compounds have been used as catalyst precursors and the subject was also recently reviewed.[23] We were interested in probing the efficacy of the presently synthesized complexes for the catalytic oxidation, with

aqueous H_2O_2, of ethylbenzene, tetraline, toluene, benzene and cumene, and we chose ethylbenzene as a reference compound to establish the best experimental conditions.

The catalytic oxidation of ethylbenzene with aqueous H_2O_2 was studied in the presence of $Cs[V^VO_2\{Hdfmp(smdt)_2\}]$ (**7**) as catalyst precursor. Generally, ethylbenzene upon oxidation of gives acetophenone, along with a small amount of benzyl alcohol.[22,25,55] However, in the present systems by far acetophenone was characterized as the major oxidation product (Scheme 2)


ethylbenzene   benzyl alcohol   acetophenone
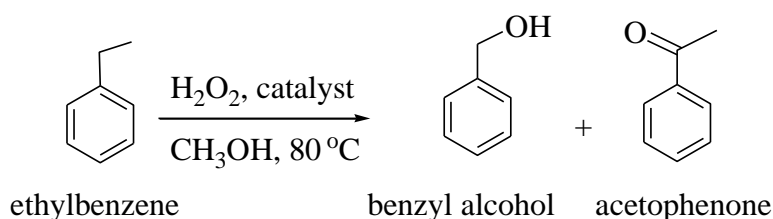
Scheme 2 Oxidative products of ethylbenzene catalyzed by the present V^VO_2-based systems.

In order to achieve the maximum oxidative products of ethylbenzene the effects of following parameters were studied in detail using $Cs[V^VO_2\{Hdfmp-(smdt)_2\}]$ (**7**) as a representative catalyst:

 i. Amount of catalyst

ii. Amount of H_2O_2

iii. Amount of solvent

iv. Temperature.

Three different amounts of catalyst precursors were added to the mixture containing ethylbenzene (1.06 g, 0.010 mol), 30% aqueous H_2O_2 (2.27 g, 0.020 mol) and 5 mL of acetonitrile and the reaction was carried out at 80 ℃. As shown in Fig. 13(a), increasing the amount of catalyst from 0.001 g to 0.002 g or to 0.003 g increases the overall percentage conversion of the substrate from 48 to 51, and 66%, respectively. The order of the selectivity of products for 0.001 g of catalyst at the end of 20 h is: acetophenone (93%) > benzylalcohol (7%); for 0.002 g and 0.003 g the selectivity remained the same. Therefore, an amount of 0.003 g of catalyst was taken for optimizing rest of the conditions.

The effect of amount of oxidant (30% aqueous H_2O_2) for the oxidation of ethylbenzene is illustrated in Fig. 13(b). Under the above conditions, with an oxidant:substrate ratio of 1:1 gave 45% conversion with 92% selectivity of acetophenone and 7% of benzylalcohol. Increasing this ratio to 2:1 improved the conversion to 65%. The conversion remained almost the same on further increasing this ratio to 3:1. At higher oxidant:substrate ratio the conversion did not increase, possibly due to dilution of the reaction mixture and/or hydrolysis of the catalyst, due to the presence of larger amounts of water. Therefore, a H_2O_2:substrate ratio of 2:1 was considered suitable to optimize other conditions. Similarly, the effect of solvent was checked considering 5, 10 and 15 mL of acetonitrile. Under the above conditions, 5 mL acetonitrile gave 63% conversion with selectivity of acetophenone (90%) and benzylalcohol (7%), while increasing the solvent volume to 10 to 15 mL did not improve the overall conversion or changed the selectivity of the products (Fig 13(c)). Under the optimized reaction conditions i.e. ethylbenzene (1.06 g, 0.010 mol), catalyst (0.003 g), 30% H_2O_2 (2.27 g, 0.020 mol) and acetonitrile (5 mL), the reaction was carried out at three different temperatures i.e. 70, 80 and 90 $^{\circ}$C. A maximum of 50 % conversion was obtained at 70 $^{\circ}$C. This conversion improved to 65% at 80 $^{\circ}$C and to 71% at 90 $^{\circ}$C, Fig 13(d).
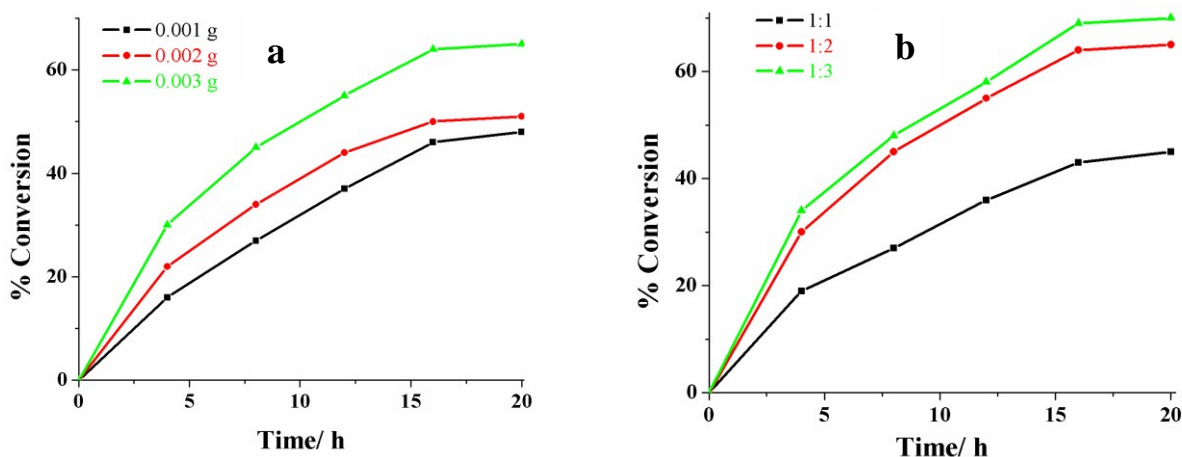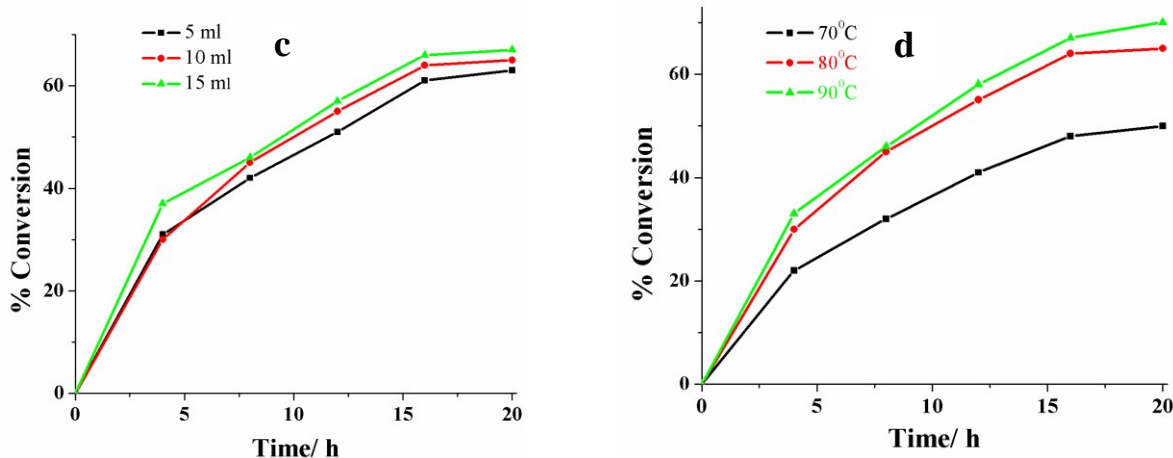
Fig. 13 Optimization of the catalytic oxidation of ethylbenzene using $Cs[V^{V}O_2\{Hdfmp\text{-}(smdt)_2\}]$ (**7**) as catalyst precursor. (a) Reaction conditions: (**a**) effect of amount of catalyst [ethylbenzene (1.06 g, 10 mmol), 30% aqueous H_2O_2 (2.27 g, 0.020 mol), acetonitrile (5 mL) and reaction temp. 80 ^{o}C]. (**b**) Effect of oxidant amount [ethylbenzene (1.06 g, 0.010 mol), catalyst (0.003 g), acetonitrile (5 mL) and reaction temp. 80 ^{o}C]. (**c**) Effect of amount solvent [ethyl benzene (1.06 g, 0.010 mol), catalyst (0.003 g), 30% aqueous H_2O_2 (2.27 g, 0.020 mol) and reaction temp. 80°C]. (**d**) Effect of temperature [ethylbenzene (1.06 g, 0.010 mol), catalyst (0.003 g), 30% aqueous H_2O_2 (2.27 g, 0.020 mol) and acetonitrile (5 mL)].

Table ESI-6 summarizes the conditions used and results obtained in the experiments described above. We chose 80 ^{o}C as the optimized reaction temperature and checked the selectivity profile along time up to 20 h; this is depicted in Fig. 14. The conversion increases with time without much change in the product selectivity.
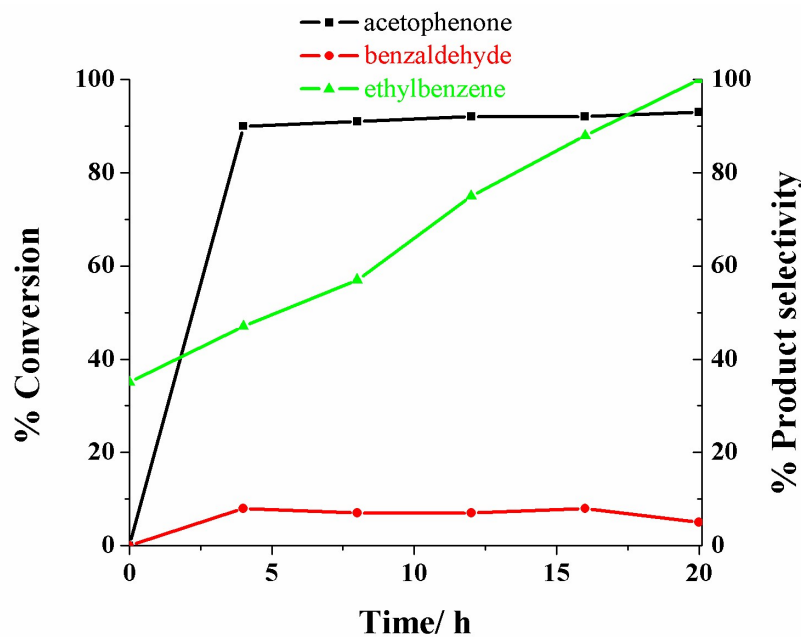
Fig. 14 Profile showing the % consumption of ethyl benzene along with the % selectivity for the formation of products using $Cs[V^VO_2\{Hdfmp\text{-}(smdt)_2\}]$ (**7**) under the optimized reaction conditions: ethylbenzene (1.06 g, 10 mmol), catalyst precursor (0.003g), 30% aqueous H_2O_2 (2.27 g, 0.020 mol), acetonitrile (5 mL) and reaction temp. 80 °C.

Using the same reaction conditions, the performance of complexes **8** and **9** was tested for the catalytic oxidation of ethylbenzene. The overall results are depicted in Table 6.

Table 6 Conversion of ethylbenzene, TOF and product selectivity at optimum reaction conditions, i.e. ethylbenzene (1.06 g, 0.010 mol), catalyst (0.003 g), 30% aqueous H_2O_2 (2.27 g, 0.020 mol), acetonitrile (5 mL) and temperature: 80 °C.

Catalyst	Conv.	TOF / h^{-1}	Selectivity (%)	
			acetophenone	benzylalcohol
$Cs[V^VO_2\{Hdfmp\text{-}(smdt)_2\}]$ (**7**)	66 %	82	92	8
$Cs[V^VO_2\{Hdfmp\text{-}(sbdt)_2\}]$ (**8**)	70 %	107	93	7
$Cs[V^VO_2\{Hdfmp\text{-}(tsc)_2\}]$ (**9**)	71 %	78	90	9

The efficacy and the selectivity for acetophenone of the present systems for the oxidation of ethylbenzene, when compared to most previous reported catalyst systems[25,56] may be considered remarkable.
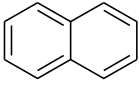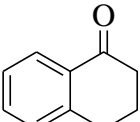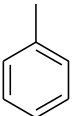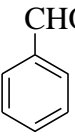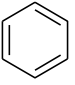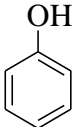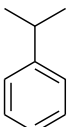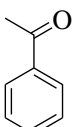
Oxidation of other arenes

Oxidation with aqueous H_2O_2 of several other aromatic compounds such as tetraline, toluene, benzene and cumene was also tested using the conditions optimized above and $Cs[V^VO_2\{Hdfmp(smdt)_2\}]$ (**7**) as catalyst precursor. Table 10 presents their conversion as well as the selectivity of key product i.e. corresponding aldehyde/ketone. Amongst them, the highest conversion was observed for tetralin (70%) and lowest for benzene (40%) whereas toluene and cumene gave approximately 60% conversion with the selectivity of the products in the range 80-90%. Interestingly the conversions were quite high and the selectivity quite satisfactory.

There are a few reports in the literature on the oxidation of the aromatic compounds of Table 7 by H_2O_2. Mimoun et al.[57] in experiments with several vanadium complexes reported low conversions and selectivity in the oxidation of toluene, with only traces of benzaldehyde or benzyl alcohol. Interestingly, the vanadate(V) oxidation of toluene to benzaldehyde in acetic acid was reported with the promoting effect obtained by addition of zirconium acetates.[58] This gave benzaldehyde as the main product, along with benzyl alcohol, benzyl acetate, benzoic acid, cresol, methylquinone, etc., but the % conversions were low, in the range 10-20 %. In another study, $V^{IV}O(acac)_2$ was used as catalyst precursor for the oxidation of toluene in glacial acetic acid, using H_2O_2 as oxidant at 90 ℃. The conversions were up to ca. 56 %. Therefore the conversions reported in Table 10 may be considered quite promising.

Several vanadium complexes were also shown to promote the hydroxylation of benzene with peroxide oxidants. Mimoun et al.[57] in experiments with several vanadium complexes reported conversions of up to 60-70%, while Conte et al. reported similar conversion values for the $VO-(O_2)$-pic system in CH_3CN[59,60] and significantly lower in ionic liquids.[26] $V^{IV}O$(tetraphenoxyphthalocyanine) was reported to be an efficient and selective catalyst for arene hydroxylation with H_2O_2, yielding (in acetonitrile at 65 ℃ for 8 h, with a 2.5 mol % catalyst loading) a conversion ca. 22 % (with 100% selectivity for phenol). In similar conditions $[V^{IV}O(acac)_2]$ afforded only 11% conversion.

Table 7 Conversion of several other aromatic compounds, their TOF and product selectivity using $Cs[V^VO_2\{Hdfmp\text{-}(smdt)_2\}]$ (**7**) as catalyst precursor. Conditions: substrate (0.010 mol), catalyst (0.003 g), aqueous 30% H_2O_2 (2.27 g, 0.020 mol), acetonitrile (5 mL) at 80 ºC.

Sl No	Substrate	Product	Time / h	Conv. (%)	Product selectivity (%)	TOF/ h^{-1}
1	Tetraline	Tetralone	8	70	80	170
2	Toluene	Benzaldehyde	20	65	78	65
3	Benzene	Phenol	20	38	90	38
4	Cumene	Acetophenone	20	61	80	61

Plausible mechanism of the reactions

Catalytic oxidations using $V^{IV}O$- or $V^{IV}O_2$-complexes as pre-catalysts and peroxides as oxidants are considered either to involve radical intermediates,[15,23,28,61] or, particularly in the case of aqueous H_2O_2, to follow pathways involving the formation of peroxido-oxidovanadium(V) intermediates, followed by its protonation at one of the peroxido O-atoms.[15,23,31,42,50,62-64] The outline made in Scheme 3 summarizes a plausible outline for the processes taking place in non-radical pathways taking $Cs[V^VO_2\{Hdfmp\text{-}(smdt)_2\}]$ (**7**) as catalyst precursor.
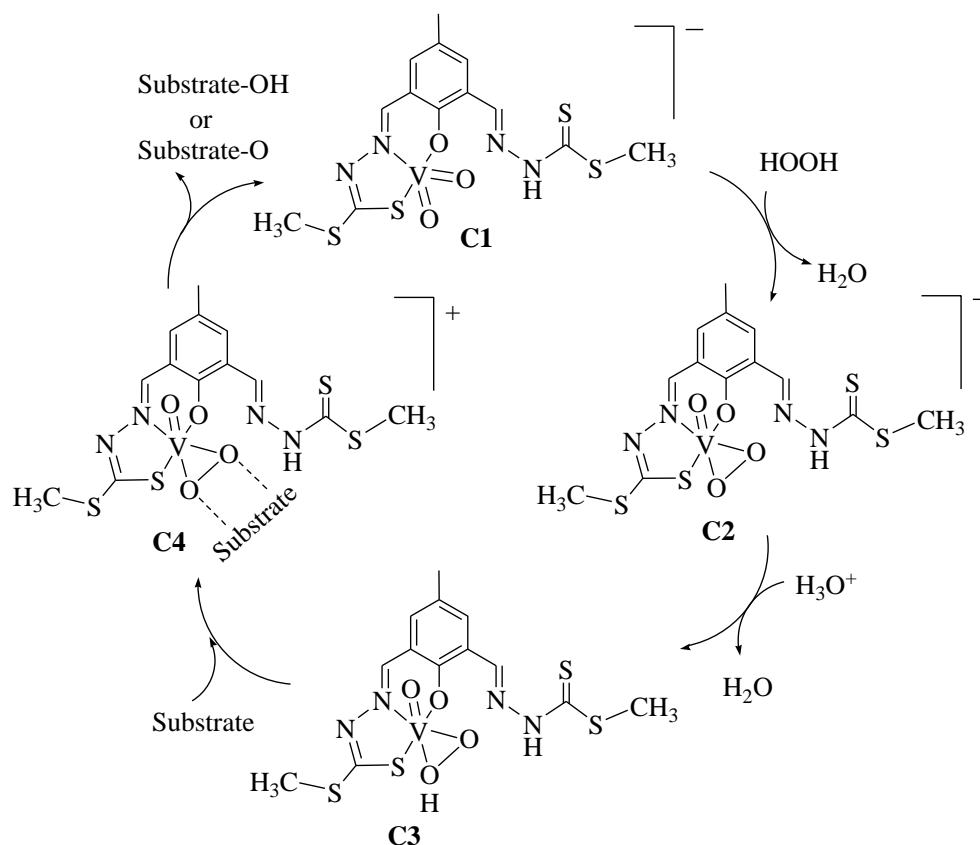
Scheme 3 Tentative outline of the major steps that may be involved in non-radical pathways of catalytic oxygen transfer reactions in the present systems, taking $[V^VO_2\{Hdfmp\text{-}(smdt)_2\}]^-$ as the pre-catalyst.

Considering radical mechanisms, these typically proceed by pathways involving both C- and O-centered radicals.[23,65] For the conversion of alcohols to the corresponding aldehyde/ketone plausible steps would be:[61]

$[V^VO_2\{Hdfmp\text{-}(smdt)_2\}]^- + H_2O_2 \rightarrow HOO^\bullet + H_3O^+ + [V^{IV}O\{Hdfmp\text{-}(smdt)_2\}]$

$[V^{IV}O\{Hdfmp\text{-}(smdt)_2\}] + H_2O_2 \rightarrow HO^\bullet + [V^VO(OH)\{Hdfmp\text{-}(smdt)_2\}]$

$[V^VO(OH)\{Hdfmp\text{-}(smdt)_2\}] + H_2O_2 \rightarrow [V^VO(OOH)\{Hdfmp\text{-}(smdt)_2\}] + H_2O$

$HO^\bullet + R(H)OH \rightarrow H_2O + R(H)^\bullet OH$

$$HOO^\bullet \ + \ R(H)OH \ \rightarrow \ H_2O_2 \ + \ R(H)^\bullet OH$$

$$[V^VO(OOH)\{Hdfmp\text{-}(smdt)_2\}] \ + \ R(H)^\bullet OH \ \rightarrow \ R(H)=O \ + \ H_2O_2 \ + \ [V^{IV}O\{Hdfmp\text{-}(smdt)_2\}]$$
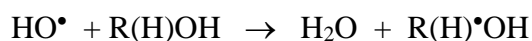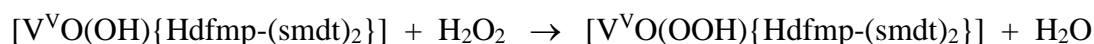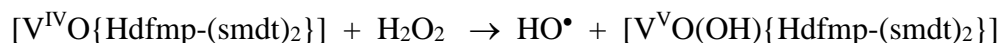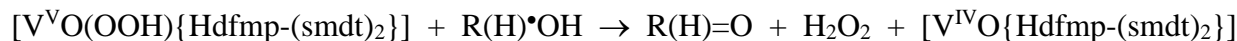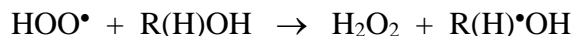
Conclusions

In this work three ligands derived from the reaction of 2,6-diformyl-4-methylphenol and S-methyldithiocarbazate, S-benzyldithiocarbazate and thiosemicarbazone were obtained. The corresponding $V^{IV}O$-complexes were prepared by their reaction with $[V^{IV}O(acac)_2]$, and K^+ and Cs^+ salts of the V^VO_2-complexes were synthesized upon oxidation of the $V^{IV}O$-compounds in the presence of either KOH or CsOH. Their characterization by analytical and spectroscopic techniques agreed with binding of the ligands to vanadium through the N-azomethine, the S- and the O-phenolic atoms.

Solutions of the complexes in either DMSO or MeOH depict ^{51}V NMR chemical shift values in the range -450 to -467 ppm, in agreement with the coordination of the soft S-donor atom, thus with a significant deshielding when compared with complexes with only N,O-donor atoms.[27] Upon addition of either t-BuOOH or aqueous H_2O_2, the formation of peroxido complexes $V^VO(O_2)(L)$ was not confirmed by ^{51}V NMR spectroscopy, but UV-Vis measurements suggest these type of complexes do form in solution.

The complexes prepared depict very good catalytic activity for the oxidation, by aqueous H_2O_2, of benzyl alcohol to benzaldehyde and ethylbenzene to acetophenone with excellent selectivity. One of the V^VO_2-complexes, $Cs[V^VO_2\{Hdfmp\text{-}(smdt)_2\}]$ (**7**), was also remarkably efficient and selective for the catalytic oxidation of several primary and secondary alcohols to the corresponding aldehyde/ketone, as well as for the oxidation of several aromatic compounds such as toluene, benzene, cumene and tetraline. The mechanisms of the catalytic reactions were not accessed, but most probably they have a radical basis.[15,23,25,26,57,60]

Acknowledgments

References

1   D. C. Crans, J. J. Smee, E. Gaidamauskas and L. Q. Yang, *Chem. Rev.*, 2004, **104**, 849–902.

2   M. Selman, C. Rousso, A. Bergeron, H. H. Son, R. Krishnan, N. A. El-Sayes, O. Varette, A. Chen, F. Le Boeuf, F. Tzelepis, J. C. Bell, D. C. Crans and J. S. Diallo, *Mol. Ther.*, 2018, **26**, 56–69.

3   J. C. Pessoa, S. Etcheverry and D. Gambino, *Coord. Chem. Rev.*, 2015, **301-302**, 24–48.

4   J. C. Pessoa, *J. Inorg. Biochem.*, 2015, **147**, 4–24.

5   K. H. Thompson and C. Orvig, *J . Inorg. Biochem.*, 2006, **100**, 1925–1935.

6   G. R. Willsky, L. H. Chi, M. Godzala, P. J. Kostyniak, J. J. Smee, A. M. Trujillo, J. A. Alfano, W.J. Ding, Z. H. Hu and D. C. Crans, *Coord. Chem. Rev.*, 2011, **255**, 2258–2269.

7   H. Sakurai, Y. Yoshikawa and H. Yasui, *Chem. Soc. Rev.*, 2008, **37**, 2383–2392.

8   E. Kioseoglou, S. Petanidis, C. Gabriel and A. Salifoglou, *Coord. Chem. Rev.*, 2015, **301**, 87–105.

9   D. C. Crans and J. J. Smee, Vanadium, in Comprehensive Coordination Chemistry II, Ed. J. A. McCleverty, T. J. Meyer, Ch 4.4, Elsevier, Amsterdam, 2004, p. 176–279.

10   M. Li, D. Wei, W. Ding, B. Baruah and D. C. Crans, *Biol. Trace Elem. Res.*, 2008, **121**, 226–232.

11   D. Gambino, *Coord. Chem. Rev.,* 2011, **255**, 2193–2203.

12   (*a*) *Vanadium compounds: Chemistry, biochemistry and therapeutic applications*, ed. V. L. Pecoraro, C. Slebodnick, B. Hamstra, D. C. Crans and A. S. Tracy, ACS Symposium Series 1998, Ch. 12; (*b*) H. Sakurai, Y. Kojima, Y. Yoshikawa, K. Kawabe and H. Yasui, *Coord. Chem. Rev.*, 2002, **226,** 187–198; (*c*) D. Rehder, J. C. Pessoa, C. F. G. C. Geraldes, M. M. C. A. Castro, T. Kabanos, T. Kiss, B. Meier, G. Micera, L. Pettersson, M. Rangel, A. Salifoglou, I. Turel and D. Wang, *J. Biol. Inorg. Chem.*, 2002, **7,** 384–396; (*d*) D. Rehder, *Inorg. Chem. Commun.*, 2003, **6,** 604–617; (*e*) M. Xie, L. Gao, L. Li, W. Liu and S. Yan, *J. Inorg. Biochem.*, 2005, **99,** 546–551.

13   M. R. Maurya, *J. Chem. Sci.,* 2011, **123**, 215–228.

14   M. R. Maurya, A. Kumar and J. C. Pessoa, *Coord. Chem. Rev.*, 2011, **255**, 2315–2344.

15   V. Conte, A. Coletti, B. Floris, G. Licini and C. Zonta, *Coord. Chem. Rev.*, 2011, **255**, 2165–2177.

16   J. A. L. da Silva, J. J. R. Fraústo da Silva and A. J. L. Pombeiro, *Coord. Chem. Rev.*, 2011, **255**, 2232–2248.

17   M. R. Maurya and J. C. Pessoa, *J. Organomet. Chem.*, 2011, **696**, 244–254.

18   M. R. Maurya, A. A. Khan, A. Azam, S. Ranjan, N. Mondal, A. Kumar, F. Avecilla and J. C. Pessoa, *Dalton Trans.*, 2010, **39**, 1345–1360.

19   M. R. Maurya, A. A. Khan, A. Azam, S. Ranjan, N. Mondal, A. Kumar and J. C. Pessoa, *Eur. J. Inorg. Chem.,* 2009, 5377–5390.

20   M. R. Maurya, C. Haldar, A. A. Khan, A. Azam, A. Salahuddin, A. Kumar and J. C. Pessoa, *Eur. J. Inorg. Chem.,* 2012, **15**, 2560–2577.

21   M. R. Maurya, M. Kumar and U. Kumar, *J. Mol. Catal A. chem.*, 2007, **273**, 133–143.

22   V. Conte and B. Floris, *Dalton Trans.*, 2011, **40**, 1419–1436.

23   R.R. Langeslay, D.M. Kaphan, C.L. Marshall, P.C. Stair, A.P. Sattelberger and M. Delferro, *Chem. Rev.*, 2019, **119**, 2128–2191.

24   N.A. Illán-Cabeza, M. N. Moreno-Carretero and J. C. Pessoa, *Inorg. Chim. Acta.*, 2005, **358**, 2246–2254.

25   M. Sutradhar, L. M. D. R. S. Martins, M. F. C. G. da Silva and A. J. L. Pombeiro, *Coord. Chem. Rev.*, 2015, **301**, 200–239.

26   V. Conte and B. Floris, *Inorg. Chim. Acta.*, 2010, **363**, 1935–1946.

27   D. Rehder, C. Weidemann, A. Duch and W. Priebsch, *Inorg. Chem.*, 1988, **27**, 584–587.

28   M. Sutradhar and A. J. L. Pombeiro, *Coord. Chem. Rev.*, 2014, **265**, 89–124.

29   G. Ambrosi, M. Formica, V. Fusi, L. Giorgi and M. Micheloni, *Coord. Chem. Rev.*, 2008, **252**, 1121–1152.

30   A. Mondal, S. Sarkar, D. Chopra, T. N. G. Row, K. Pramanik and K. K. Rajak, *Inorg. Chem.*, 2005, **44**, 703–708.

31   M. R. Maurya, C. Haldar, A. Kumar, M. L. Kuznetsov, F. Avecilla and J. C. Pessoa, *Dalton Trans.*, 2013, **42**, 11941–11962.

32   R. A. Rowe and M. M. Jones, *Inorg. Synth.*, 1957, **5**, 113–116.

33   R. R. Gagne, C. L. Spiro, T. J. Smith, C. A. Hamann, W. R. Thies and A. D. Shiemke, *J. Am. Chem. Soc.*, 1981, **103**, 4073–4081.

34   M. A. Ali and M. T. H. Tarafder, *J. Inorg. Nucl. Chem.*, 1977, **39**, 1785–1791.

35   M. Das and S. E. Livingstone, *Inorg. Chim. Acta.*, 1976, **19**, 5–10.

36   A. Rockenbauer and L. Korecz, *Appl. Magn. Reson.*, 1996, **10**, 29–43.

37   L. Vilas Boas and J. C. Pessoa, "Vanadium" in *Comprehensive Coordination Chemistry*, ed. G. Wilkinson, R.D. Gillard and J.A. McCleverty, Pergamon, Oxford, 1987, Vol. 3, pp. 453-583.

38   M. R. Maurya, *Coord. Chem. Rev.*, 2003, **237**, 163–181.

39   K. Wüthrich, *Helv. Chim. Acta*, 1965, **48**, 1012–1017.

40   N. D. Chasteen, in: *Biological Magnetic Resonance* (Ed.: J. Reuben), Plenum, New York, **1981**, p. 53.

41   M. R. Maurya, A. A. Khan, A. Azam, S. Ranjan, N. Mondal, A. Kumar and J. C. Pessoa, *Eur. J. Inorg. Chem.*, **2009**, 5377–5390.

42   D. Rehder, Bioinorganic Vanadium Chemistry, John Wiley & Sons, New York, 2008, pp. 53-71.

43   J. Tasiopoulos, A. N. Troganis, A. Evangelou, C. P. Raptopoulou, A. Terzis, Y. Deligiannakis and T. A. Kabanos, *Chem. Eur. J.*, 1999, **5**, 910–921.

44   D. Rehder, in: P.S. Pregosin (Ed.), Transition Metal Nuclear Magnetic Resonance, Elsevier, New York, 1991, p. 1.

45   A. Tracey, G. R. Willsky and E. S. Takeuchi, Vanadium. Chemistry, Biochemistry, Pharmacology and Practical Applications, CRC Press, Boca Raton, 2007, pp. 8–12.

46   Saswati, P. Adão, S. Majumder, S. P. Dash, S. Roy, M. L. Kuznetsov, J. C. Pessoa, C. S. B. Gomes, M. R. Hardikar, E. R. T. Tiekink and R. Dinda, *Dalton Trans.*, 2018, **47**, 11358–11374.

47   M.R. Maurya, U. Kumar, I. Correia, P. Adao and J. C. Pessoa, *Eur. J. Inorg. Chem.*, 2008, 577–587.

48   M.R. Maurya, N. Chaudhary, A. Kumar, F. Avecilla and J. C. Pessoa, *Inorg. Chim. Acta.*, 2014, **420**, 24–38.

49   M.R. Maurya, A. Arya, U. Kumar, A. Kumar, F. Avecilla and J. C. Pessoa, *Dalton Trans.*, 2009, 9555–9566.

50 (*a*) M.R. Maurya, A. Arya, A. Kumar, J. C. Pessoa, *Dalton Trans*., 2009, 2185–2195; (*b*) M.R. Maurya, A. Arya, A. Kumar, M.L. Kuznetsov, F. Avecilla and J. C. Pessoa, *Inorg. Chem*., 2009, **49**, 6586–6600.

51 V. Conte, F. Di Furia and S. Moro, *J. Mol. Catal*., 1994, **94**, 323–333.

52 M.S. Reynolds and A. Butler, *Inorg. Chem*., 1996, **35**, 2378–2383.

53 G. J. Colpas, B.J. Hamstra, J.W. Kampf and V.L. Pecoraro, *J. Am. Chem. Soc*., 1996, **118**, 3469–3478.

54 V. K. Bansal, P. P. Thankachan and R. Prasad, *Appl. Catal*. A., 2010, **281**, 8–17.

55 (a) M. Bagherzadeh, M. Amini, A. Ellern and L. K. Woo, *Inorg. Chem. Commun*., 2012, **15**, 52–55. (b) H. H. Monfared, S. Kheirabadi, N. A. Lalami and P. Mayer, *Polyhedron*, 2011, **30**, 1375–1384.

56 M.R. Maurya, A. Arya, P. Adao and J. C. Pessoa, *Appl Catal. A: Gen*., 2008, 351, 239–252.

57 H. Mimoun, L. Saussine, E. Daire, M. Postel, J. Fischer and R. Weiss, *J. Am. Chem. Soc*., 1983, **105**, 3101−3110.

58 X. Wang, X. Cao, X. Hu, G. Li, L. Zhu and C. Hu, *J. Mol. Catal. A: Chem*., 2012, **357**, 1–10.

59 M. Bianchi, M. Bonchio, V. Conte, F. Coppa, F. Di Furia, G. Modena, S. Moro and S. Standen, *J. Mol. Catal*., 1993, **83**, 107–116.

60 M. Bonchio, V. Conte, F. Di Furia, G. Modena and S. Moro, *J. Org. Chem*., 1994, **59**, 6262−6267.

61 (*a*) M. Sutradhar, L. M. D. R. S. Martins, M. F. C. G. da Silva and A. J. L. Pombeiro, *Appl. Catal. A-Gen*., 2015, **493**, 50–57; (*b*) M. Sutradhar, L. M. D. R. S. Martins, S.A.C. Carabineiro, M. F. C. G. da Silva, J. G. Buijnsters, J. L. Figueiredo and A. J. L. Pombeiro, *Chem. Cat. Chem*., 2016, **8**, 2254-2266; (*c*) M. Sutradhar, L. M. D. R. S. Martins, T. R. Barman, M. L. Kuznetsov, M. F. C. G. da Silva and A. J. L. Pombeiro, *New J. Chem.*, 2019, **43**, DOI: 10.1039/c9nj00348g.

62 (*a*) M. L. Kuznetsov and J. C. Pessoa, Dalton Trans., 2009, 5460–5468; (*b*) P. Adao, M. L. Kuznetsov, S. Barroso, A.M. Martins, F. Avecilla and J. C. Pessoa, *Inorg. Chem*., 2012, **51**, 11430–11449.

New Journal of Chemistry Accepted Manuscript

63   (*a*) M. R. Maurya, B. Uprety, F. Avecilla, P. Adao, M. L. Kuznetsov and J. C. Pessoa, *Eur. J. Inorg. Chem.*, 2017, 3087–3099; (*b*) P. Adao, M. R. Maurya, U. Kumar, F. Avecilla, R. T. Henriques, M. L. Kusnetsov, J. C. Pessoa and I. Correia, *Pure Appl. Chem.*, 2009, **81**, 1279–1296.

64   (*a*) G. B. Shul'pin, Y. N. Kozlov, G. V. Nizova, G. Suss-Fink, S. Stanislas, A. Kitaygorodskiy and V. S. Kulikova, *J. Chem. Soc., Perkin Trans. 2*, 2001, 1351−1371; (*b*) C. J. Schneider, J. E. Penner-Hahn and V. L. Pecoraro, *J. Am. Chem. Soc.*, 2008, **130**, 2712–2713; (*c*) G. Zampella, P. Fantucci, V. L. Pecoraro and L. De Gioia, *J. Am. Chem. Soc.*, 2005, **127**, 953–960; (*d*) V. Conte, O. Bortolini, M. Carraro and S. Moro, *J. Inorg. Biochem.,* 2000, **80**, 41–49.

65   (*a*) L. M. Slaughter, J. P. Collman, T. A. Eberspacher and J. I. Brauman, *Inorg. Chem.*, 2004, **43**, 5198–5204; (*b*) J. M. Mattalia, B. Vacher, A. Samat and M. Chanon, *J. Am. Chem. Soc.*, 1992, **114**, 4111–4119.

New Journal of Chemistry Accepted Manuscript

Table of Contents

New thiosemicarbazide and dithiocarbazate based oxidovanadium(IV) and dioxidovanadium(V) complexes. Reactivity and catalytic potential

Mannar R. Maurya, Bithika Sarkar, Amit Kumar, Nádia Ribeiro, Aistè Miliute and J. C. Pessoa

The new thiosemicarbazide and dithiocarbazate based vanadium complexes depict remarkable catalytic potential for oxidation of alcohols and simple arenes.